Deliverable D3.2: Radio Technology Performance Report

Version: V1.0

March 6, 2020

Revision history

Revision	Date	Description
0.5	October 31, 2019	First version for review
0.9	January 30, 2020	Final draft awaiting final comments
1.0	March 6, 2020	First version

Contents

1 Scope

The present document provides performance evaluation of C-V2X and ITS-G5 link level and C-V2X system performance. Chapter 4 presents the link level simulators for C-V2X and ITS-G5, followed by simulation results. Chapter 5 then presents the system simulator for the C-V2X mode 3, where the car to car communication is completely scheduled by eNBs of the LTE network, follow by the discussion of simulation results. The final chapter 6 contains a summary and conclusion.

2 References

[1]   Wang Min, Martin Winbjörk, Zhang Zhang, Ricardo Blasco, Hieu Do, Stefano Sorrentino, Marco Belleschi, Yunpeng Zang: Comparison of LTE and DSRC-Based Connectivity for Intelligent Transportation Systems, IEEE VTC 2017 spring, Sidney, Australia, June 2017"

[2]   3GPP TR 36.885 V14.0.0 (2016-06), Study on LTE-based V2X Services (Release 14)

[3]   Bultitude, Yvo de Jong, and Terhi Rautiainen. "IST-4-027756 WINNER II D1. 1.2 V1. 2 WINNER II Channel Models." EBITG, TUI, UOULU, CU/CRC, NOKIA, Tech. Rep., Tech. Rep (2007).

[4]   Abdelgader, Abdeldime MS, and Wu Lenan. "The physical layer of the IEEE 802.11 p WAVE communication standard: the specifications and challenges." *Proceedings of the world congress on engineering and computer science*. Vol. 2. 2014

[5]   ITU-R M. 1225, *Guidelines for Evaluation of Radio Transmission Technologies for IMT-2000* (1997)

[6]   Paul Alexander, David Haley, Alex Grant , "Cooperative Intelligent Transport Systems: 5.9-GHz Field Trials," Proceedings of The IEEE Volume:99 , Issue 7, July 2011

3 Definitions and Abbreviations

3.1 Definitions

PC5 transport: Transmission of V2X data from a source UE (e.g., a vehicle) to a destination UE (e.g., another vehicle, road infrastructure, a pedestrian, etc.) via ProSe Direct Communication over the PC5 interface between the UEs (sidelink).

Road Side Unit (RSU): An entity supporting V2I Service that can transmit to, and receive from a UE using V2I application. RSU is implemented in an eNB or a stationary UE.

Uu transport: Transmission of V2X data from a source UE (e.g., a vehicle) to a destination UE (e.g., another vehicle, road infrastructure, a pedestrian, etc.) via the eNB over the conventional Uu interface (uplink and downlink).

V2I Service: A type of V2X Service, where one party is a UE and the other party is an RSU both using V2I application.

V2N Service: A type of V2X Service, where one party is a UE and the other party is a serving entity, both using V2N applications and communicating with each other via cellular network (e.g. LTE or 5G).

V2V Service: A type of V2X Service, where both parties of the communication are UEs using V2V application. For this service both vehicle-side UEs represent V-ITS-S.

3.2 Abbreviations

3GPP	3rd Generation Partnership Project
5G	5th Generation
CAM	Cooperative Awareness Message
C-ITS	Cooperative Intelligent Transport Systems
C-V2X	Cellular V2X
DSRC	Dedicated Short Range Communications
EEBL	Emergency Electronic Brake Light (use case)
EIRP	Equivalent Isotropically Radiated Power
ETSI	European Telecommunications Standards Institute
IEEE	Institute of Electrical and Electronics Engineers
ITS	Intelligent Transport System
ITS-G5	ITS using 5 GHz frequency band
KPI	Key Performance Indicators
L2S	Link-to-System
LLS	Link Level Simulator
LTE	Long Term Evolution
MAC	Media Access Control (layer)

MCS	Modulation and Coding Scheme
PC5	ProSe Communication reference point 5
PHY	Physical (layer)
ProSe	Proximity-based Services
PRB	Physical Resource Block
PRR	Packet Reception Rate
PSDU	PHY Service Data Unit
REFSENS	Reference Sensitivity
RSU	Road Side Unit
SCI	Sidelink Control Information
SINR	signal-to-interference and noise ratio
SNR	signal-to-noise ratio
TBS	Transport Block Size
UE	User Equipment
V2I	Vehicle to Infrastructure
V2N	Vehicle to Network
V2V	Vehicle to Vehicle
V2X	Vehicle to Everything

4 Link Level Simulation Results

Link level simulation entails communication modeling of a single radio link which in turn is performed by modeling the whole physical layer processing chain from transmitter to receiver. Programs written for this purpose are called Link Level Simulators (LLSs). In this section, we consider the two candidate technologies – ITS-G5 and C-V2X and show their performance in terms of Block Error Rate (BLER) versus SNR.

4.1 ITS-G5

The 802.11p equivalent in the European C-ITS stack covering PHY and MAC layers is termed as ITS-G5. Similar to its US counterpart, DSRC, it also operates in the 5.9 GHz band. The packet structure of 802.11p is shown in Figure 4-1.
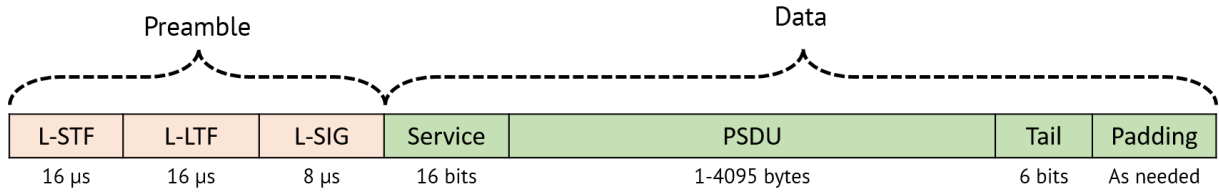
L-STF	L-LTF	L-SIG	Service	PSDU	Tail	Padding
16 µs	16 µs	8 µs	16 bits	1-4095 bytes	6 bits	As needed

Figure 4-4-1: 802.11p Packet Structure

Each transmission instance starts with a preamble that consists of three fields –

1. Legacy Short Training Field (L-STF) that is used for packet detection, coarse frequency correction, and automatic gain control
2. Legacy Long Training Field (L-LTF) that is used for fine frequency correction, fine symbol timing offset correction and pilot based channel estimation.
3. Legacy Signal field (L-SIG) contains packet information for the received configuration such as MCS scheme used and the length of the PSDU.
4. The service field consists of 16 zeros to initialize the data scrambler
5. PSDU contains the actual user data
6. Tail bits are used to terminate the convolutional code
7. The padding bits are added to ensure an integer number of symbols.
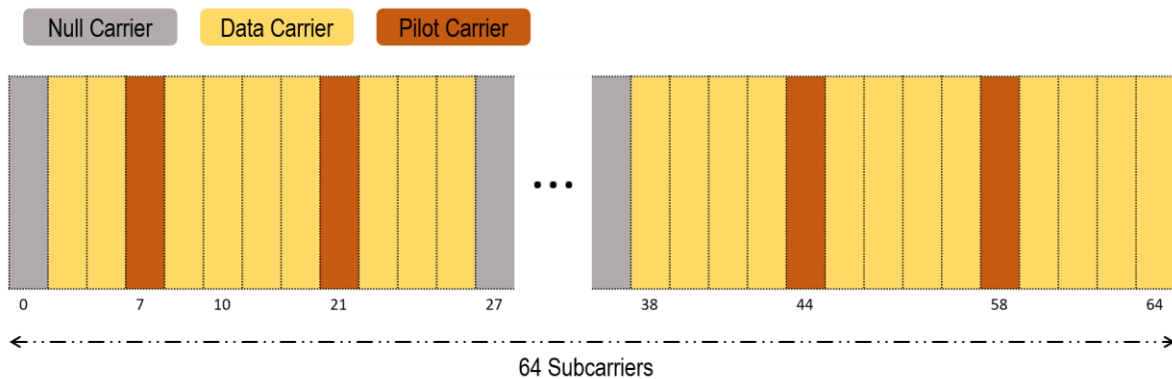
Figure 4-2: Subcarrier arrangement in ITS-G5

The PHY layer OFDM structure of 802.11p is outlined Figure 4-3. It consists of 64 frequency subcarriers out of which 52 useful subcarriers are used for data and pilot symbols and the remaining 12 are null carriers that carry no data. The null carriers occupy the central 11 subcarriers and the 0th subcarrier. Out of the remaining 52 subcarriers, the pilot symbols occupy 4 subcarriers with indices 7, 10, 44 and 58. The remaining 48 subcarriers are used for data [4].

The Tx-RX chain for 802.11p link level is highlighted in Figure 4.3. Matlab's WLAN system toolbox was used in order to build the processing pipeline. For further information regarding the algorithms used for receiver processing, please refer to Matlab's WLAN toolbox documentation.

Figure 4-3: Tx-Rx Chain for ITS-G5

The preamble is generated first along with the data and is OFDM modulated on a 10MHz bandwidth. The transmitted signal is filtered through a fading channel and AWGN noise is added to it. The receiver operations consist of
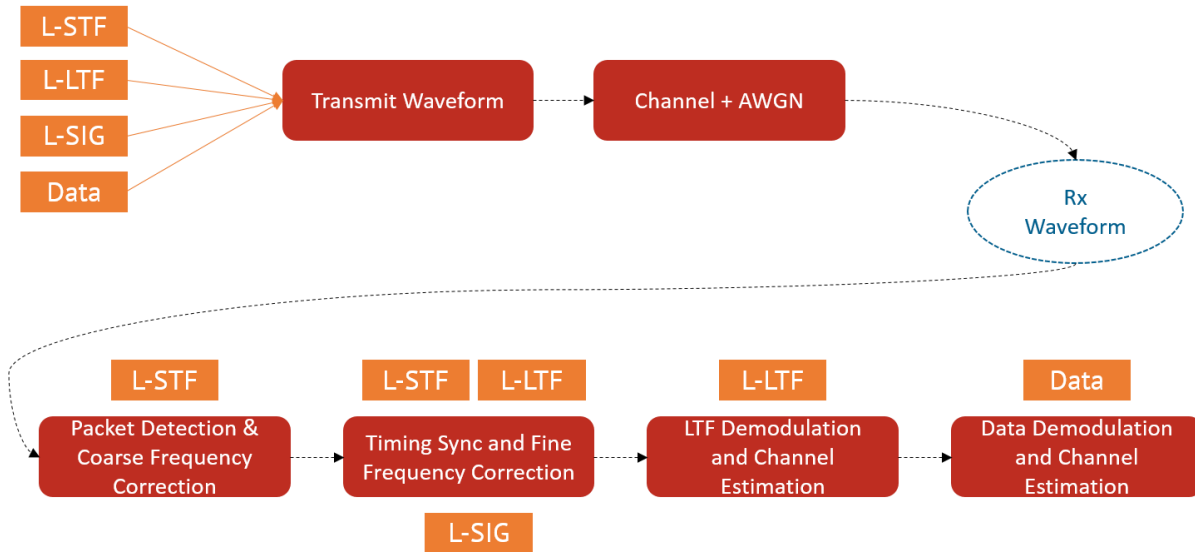
1. Packet detection, estimation of coarse packet offset and coarse frequency correction using the STF
2. Fine packet offset estimation, fine frequency offset correction and fine symbol timing offset correction using the complete preamble
3. Demodulation of LTF and channel estimation using the pilot symbols
4. The constructed channel coefficient matrix is used to demodulate, equalize and decode the PSDU data

ITS-G5 supports different MCS schemes as outlined in Table 4-1.

Table 4-4-1: Simulation Configurations – ITS-G5

MCS	MODULATION	CODING RATE	CODED BITS PER OFDM SYMBOL	DATA RATE (MBPS)
0	BPSK	1/2	48 (24 data bits)	3
1	BPSK	3/4	48 (36 data bits)	4.5
2	QPSK	1/2	96 (48 data bits)	6
3	QPSK	3/4	96 (72 data bits)	9
4	16QAM	1/2	192 (96 data bits)	12
5	16QAM	3/4	192 (144 data bits)	18
6	64QAM	2/3	288 (192 data bits)	24
7	64QAM	3/4	288 (216 data bits)	27

4.2 C-V2X

The general structure of the Transmit Receive Chain for link level simulations of C-V2X is given in Figure 4-4.

At first, the high level simulation configuration is set which consists of parameters such as allocated channel bandwidth, allocated number of PRBs for the sidelink transmission along with the transport block size and the modulation methods used. In the next step, the resource pools are created as per the allocated resource blocks and are mapped for transmission.

4.2.1 Control Channel Processing

The control channel processing consists of the steps described in the following subsections.

4.2.1.1 SCI message encoding

For V2C transmission a 'Format 1' SCI message is generated that consists of information such as the modulation & coding scheme (MCS), Resource Indication Value (RIV), the time gap between initial transmission and retransmission and the retransmission index (0 in case of initial transmission and 2 in case of first retransmission). The generated binary message is encoded using a convolutional encoder followed by rate matching and interleaving, and a 16 bit CRC is attached to the encoded message. After generating the binary code word, next processing steps involve PSCCH-specific scrambling, QPSK modulation and SC-FDMA transform precoding to generate symbols. Finally, the generated PSCCH symbols and are cyclic shifted with a random value chosen from $\{0, 3, 6, 9\}$.

The 16 bit CRC is then converted into a decimal number and this value is referred to as V2X scrambling identity (NXID). It is used as the initialization value for generating the Gold sequence which is in turn used for scrambling the user data. This effectively means that the receiver would be able to decode the data message if and only if it has decoded the SCI message successfully and recovered the 16 bit CRC remainder.
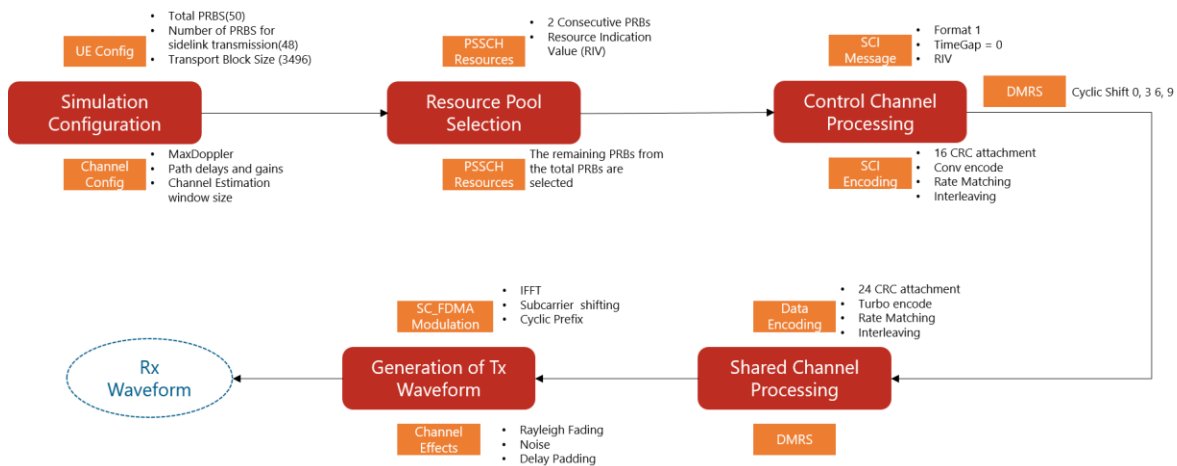

Figure 4-4: C-V2X Transmission Chain

4.2.1.2 DMRS Encoding

Demodulation Reference Signals are useful for coherent demodulation. 4 DMRS symbols are transmitted in each subframe at the indices $\{2, 5, 8, 11\}$.

4.2.2 Shared Channel Processing

The sidelink shared channel (SL-SCH) transport channel processing includes type-24A CRC calculation, code block segmentation (including type-24B CRC attachment, if present), turbo encoding, rate matching with redundancy version (RV), code block concatenation, and PUSCH interleaving. The generated codeword is then scrambled, modulated using either QPSK or 16QAM. Finally, transform precoding is applied to the modulated symbols which is a form of Discrete Fourier Transformation (DFT) to spread the data in order to reduce Peak-to-Average Power Ratio (PAPR). Similar to the control channel, DMRS symbols are added and transmitted alongside the data symbols using the four SC-FDMA symbols allocated to DMRS in a PSSCH subframe.

4.2.3 SC-FDMA Modulation

All the symbols are then mapped to the sidelink resource grid followed by SC-FDMA modulation to create the time domain waveform. The generated time domain waveform is then passed through a transmission channel model as defined in Section 4.3.

4.2.4 Receive Chain

The receive chain basically performs the inverse operations of the transmit chain and is given in Figure 4-5 below.
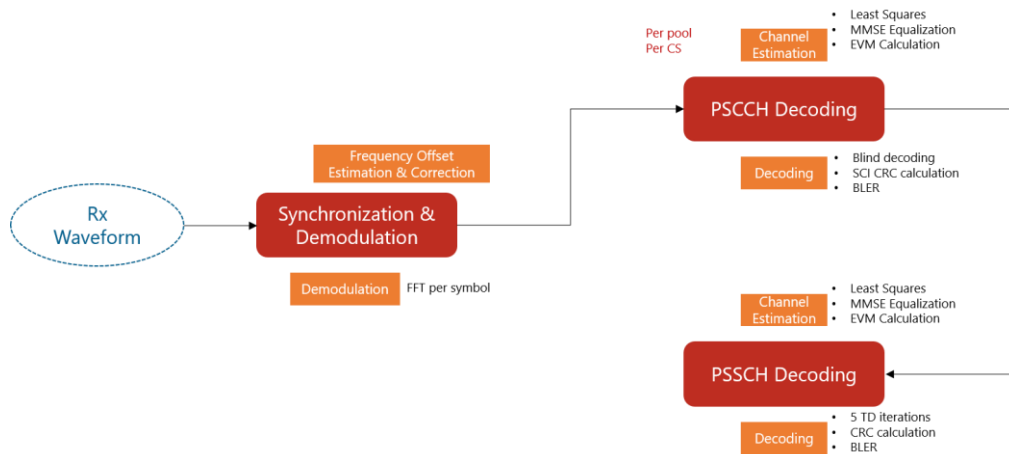

Figure 4-5: C-V2X Receive Chain

For each resource pool as configured in the resource pool selection, the receiver tries to perform a blind decoding of the control information by iterating over all possible cyclic shift values. For each selected cyclic shift, the receiver first corrects the frequency offset, demodulates the SC-FDMA time domain symbols to recover the resource grid. This is followed by MMSE channel estimation method using a cubic interpolation over pre specified time and frequency windows. The effect of the channel is equalized by dividing the received grid with that of the estimated channel grid. After this, the control symbols are extracted and are then decoded (by performing the inverse operations) to recover the SCI message. If the SCI decoding is successful, then the receiver converts the 16 bit CRC checksum into a decimal NXID is used to proceed with decoding the data message. If the decoding is not successful, it means that the shared data is also discarded.

After decoding the SCI message and recovering the NXID, the receiver proceeds with decoding the data. Similar operations (channel estimation, equalization and turbo decoding) are performed to recover the data block.

The different MCS schemes that are used for C-V2X are outlined in Table 4-2. Here, we consider a bandwidth of 10 MHz that corresponds to 50 PRBs. Since 2 PRBs are used for control message, there are 48 PRBs remaining for the user data transmission. The effective coding rate is then calculated as follows

$$Effective\ Coding\ Rate = \frac{TBS}{NPRB * 12 * Q_m * N_{sym}}$$

Where TBS is the transport block size given in Table 4-2, $NPRB$ is the number of PRBs used for data transmission (48), Q_m is the bits/symbol (2 for QPSK and 4 for 16QAM) and N_{sym} is the number of useful OFDM symbols used for carrying data. Out of 14 OFDM symbols per subframe, 4 are used for DMRS symbols and the remaining 10 are used for carrying data. However, before SC-FDMA modulation, the last OFDM symbol is set to 0 in accordance with 3GPP specification. Therefore, the total useful symbols per subframe becomes 9. These values are used for calculating the effective coding rate for the different MCS schemes in C-V2X.

Table 4-4-2 shows the modulation and coding schemes (MCS) together with the transport block sizes (TBS).

Table 4-4-2: MCS and transport block sizes (TBS)

MCS Scheme	Modulation	TBS	Effective Coding Rate
0	QPSK	1320	0.127
1	QPSK	1736	0.167
2	QPSK	2152	0.207
3	QPSK	2792	0.269
4	QPSK	3496	0.337
5	QPSK	4264	0.411
6	QPSK	4968	0.479
7	QPSK	5992	0.577
8	QPSK	6712	0.647
9	QPSK	7480	0.721
10	QPSK	8504	0.820
11	16QAM	8504	0.410
12	16QAM	9528	0.459
13	16QAM	11064	0.533
14	16QAM	12216	0.589
15	16QAM	13536	0.652
16	16QAM	14688	0.708
17	16QAM	15840	0.763
18	16QAM	17568	0.857
19	16QAM	19080	0.920
20	16QAM	20616	0.994

4.2.5 Resource Pools

In contrast to 802.11p, the C-V2X sidelink transmissions are scheduled to operate side by side with the Uplink transmissions and only in a subset of subcarriers. Hence, new measures for resource allocation and transmission scheduling are required. This is achieved by means of Resource Pools (RP), a set of resources assigned to the sidelink operation. It consists of a set of sub-frames and resource blocks within. The physical resources (sub-frames and resource blocks) associated with a given pool are partitioned into a sequence of repeating 'hyperframes' known as PSSCH periods, also referred to as the Scheduling Assignment (SA) period and Sidelink Control (SC) period. Within a PSSCH period there are separate sub-frame pools and resource block pools for control and data. The PSCCH} carries Sidelink Control Information (SCI) messages, which describe the dynamic transmission properties of the PSSCH that follow it. The receiving UE searches all configured PSSCH resource pools for SCI transmissions of interest to it.

Figure 4-6 illustrates an example sidelink hyperframe for a bandwidth of 10 MHz and a PSSCH period of 40 ms. Within a PSSCH period, the actual sidelink transmissions can be found on any two subframes (for first transmission and retransmission) given by the subframe bitmap. For the considered bandwidth of 10 MHz, there are 50 PRBs that are divided into 10 sub-pools each consisting of 5 contiguous PRBs. A UE can use one or multiple sub-pools for transmission as specified by higher layer messages. For retransmission (1 blind retransmission is supported by default), the UE can use the same set of sub-pools as the first transmission and use different sub-pools. In our example, the UE uses RP-1 for the first transmission and RP-2 for the retransmission.

The SCI message always spans 2 PRBs which is succeeded by the data message. For the given example, a data message spanning over 3 PRBs is assumed. The content of each message is also illustrated in the figure. In line with the LTE specification, each PRB consists of 12 subcarriers in the frequency domain and 14 OFDM symbols in the time domain. Symbols 2, 5, 8 and 11 are used for transmitting DMRS that are used for frequency correction and channel estimation. The remaining 10 symbols are used to carry the actual data.
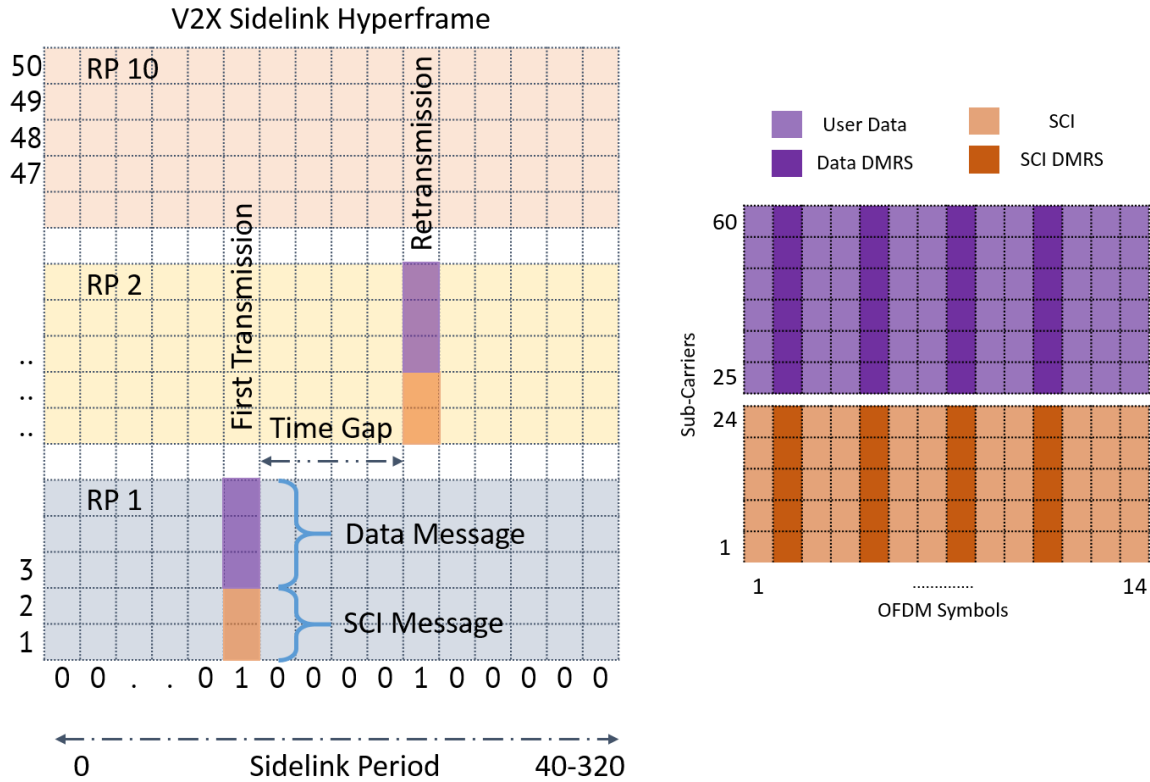
Figure 4-6: Example C-V2X Sidelink Hyperframe

4.3 Link Level Performance Comparison

In this section, we compare the link level performance between ITS-G5 and C-V2X for different channel models. We first start with AWGN channel and extend our evaluation to fading channel models that are specified by ITU and channel models that have been derived from extensive V2V field trials (see Section 4.3.2.3).

4.3.1 Performance Comparison over AWGN Channel

Figure 4-7 shows the BLER performance over AWGN channel for ITS-G5. Figure 4-8 and Figure 4-9 shows the BLER performance over AWGN channel for C-V2X with and without blind retransmission respectively. For the C-V2X curves, the QPSK schemes are highlighted in solid lines and the 16QAM schemes are highlighted with dotted lines.

For the simulation, the MCS schemes outlined in Table 4-4-1 and Table 4-4-2 were considered for both technologies. In order to have a close performance comparison, we take a look at MCS schemes 2, 3, 4, 5 for ITS-G5 that includes QPSK and 16QAM with coding rates ½ and ¾. In the case of C-V2X, the corresponding closest schemes would be **7, 9, 13 and 17** (highlighted in **thicker red**). For the case of no retransmission, the C-V2X shows a performance gain between 4 - 5 dB over ITS-G5. This is due to the use of turbo coding used in C-V2X which also makes the BLER curves steeper compared to ITS-G5.

Due to the use of retransmissions, the SNR gain is theoretically doubled. This effect is seen in the form of shifted SNR points by 3 dB to the left as seen in Figure 4-9. However, the retransmission effect is more pronounced for higher coding rates than the lower coding rates. For example, for MCS 0, there is almost a 3 dB gain whereas for MCS 10 the gain is 6 dB. Similarly, for the case of 16QAM, MCS 11 has a gain of 3 dB whereas MCS 20 has gain of almost 8 dB. This is also the reason behind the big gap between QPSK and 16QAM schemes. For no retransmission, MCS 10 (QPSK) and MCS 11 (16QAM) have almost the same BLER curve due to the same transport block size.
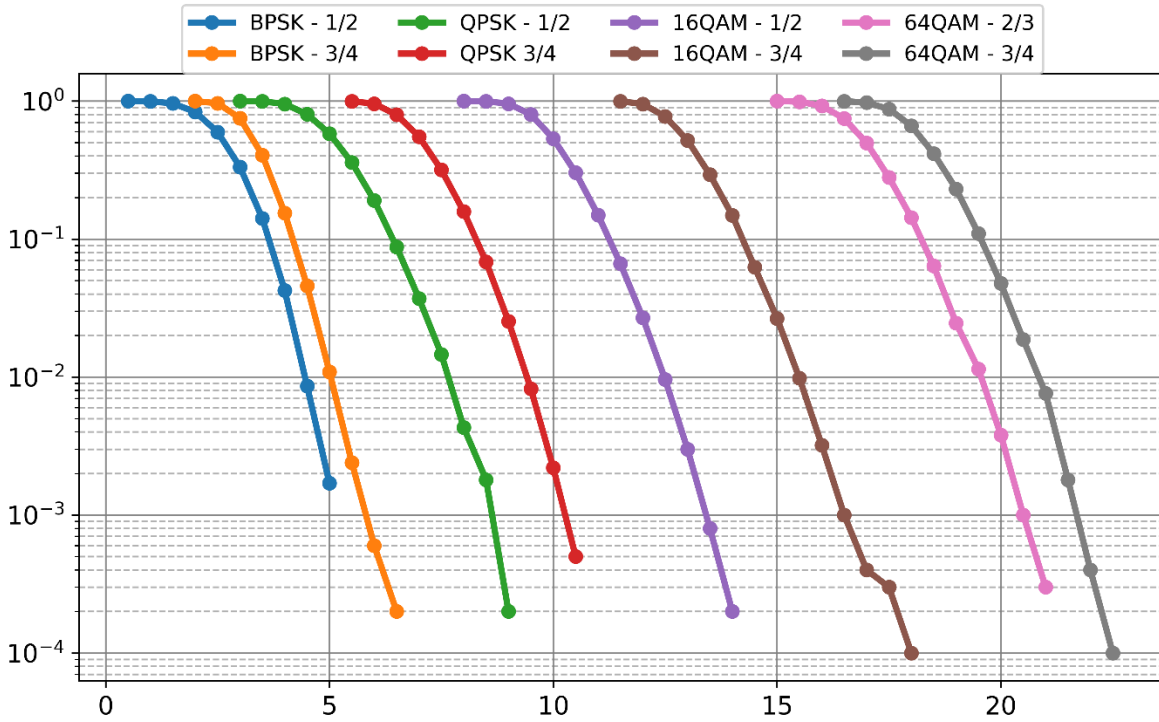

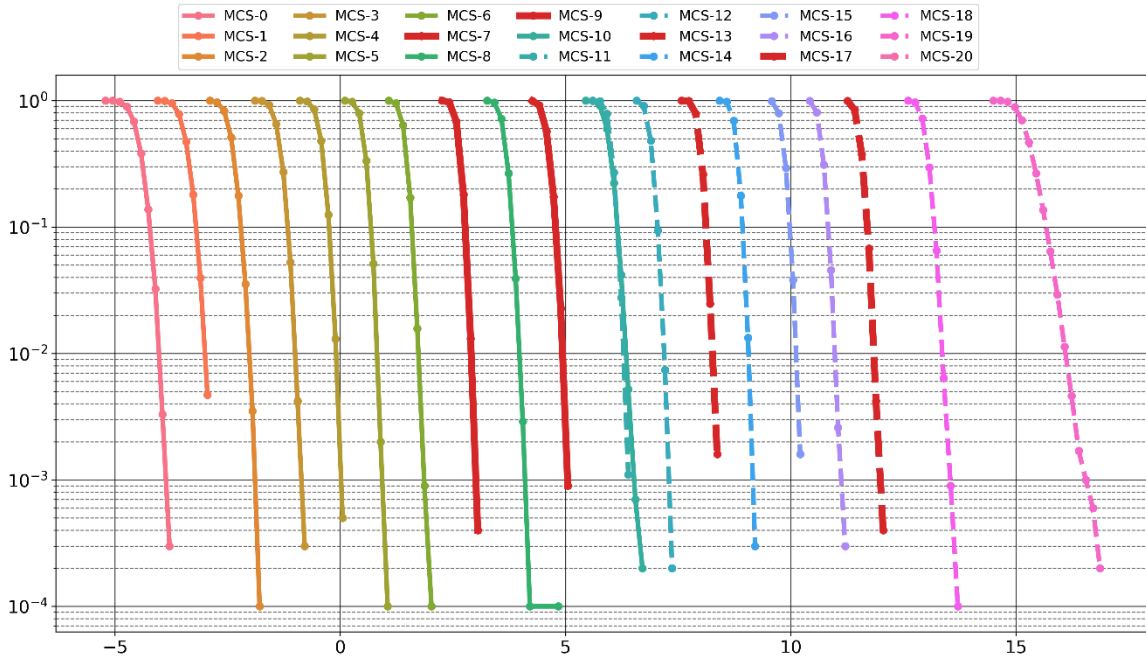*Figure 4-7: SNR Versus BLER for ITS-G5 (AWGN)*

Figure 4-8: SNR Versus BLER for C-V2X (No Retransmission)
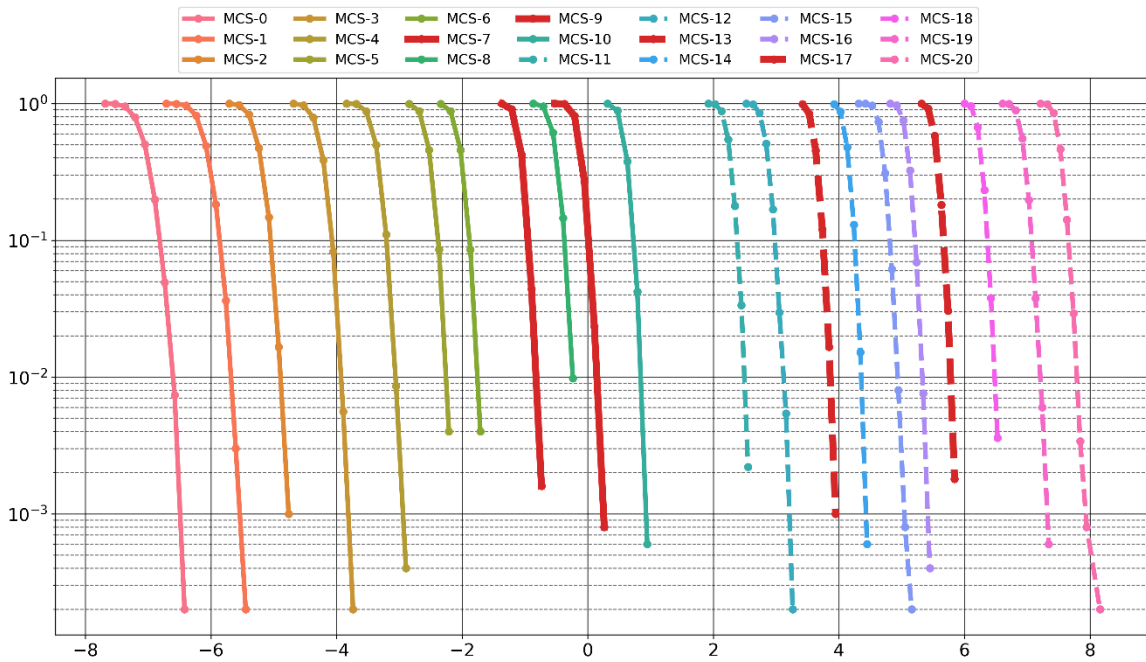

Figure 4-9: SNR Versus BLER for C-V2X (1 Blind Retransmission)

4.3.2 Performance over Fading Channels

In order to compare the link level performance of ITS-G5 with C-V2X, a set of high level parameters need to be selected in order to establish a common ground. The following common assumptions were made:

1. Bandwidth – 10 MHz

2. Only single transmission (i.e. no retransmission)
3. MCS Schemes used – QPSK 1/2, QPSK 3/4, 16QAM 1/2, 16QAM 3/4
4. Antenna Configuration – 1 Tx and 1 Rx
5. Packet size – 300 bytes (2400 bits)

At the PHY layer, ITS-G5 supports any packet size whereas the PHY layer packet in C-V2X, i.e. the transport block, is limited to a few values, due to finite values at the rate matcher. Hence, in case of C-V2X, it is not possible to set the packet size to exactly 2400 bits since the MCS scheme has to be selected from a list of predefined values based on the available Physical Resource Blocks (PRBs). Moreover, the coding rate is always slightly on the lower/higher side due to rate matching and the tail bits added to the turbo encoder. Hence the following configurations are used in order to keep the modulation and coding rates as close as possible to that of ITS-G5 and not violating the intended packet size too much.

Table 4-3: C-V2X Packet Sizes

MCS SCHEME	MCS INDEX	TBS	PRBS	EFFECTIVE CODING RATE
QPSK 1/2	7	2472	20	0.578
QPSK 3/4	9	2856	18	0.741
16QAM 1/2	13	2728	12	0.525
16QAM 3/4	17	2600	8	0.759

There are different channel models available for V2V communications. Most significant of them are the channel models derived by the C-ITS field trials and the ones proposed by ITU.

4.3.2.1 ITU Channel Models - SISO Channels

The specification ITU-R M.1225 [5] specifies three different test environments: Indoor office, outdoor-to-indoor pedestrian and vehicular-high antenna. For the vehicular test environment, low (Channel A) and medium (Channel B) delay spreads have been defined with 6 channel taps and an RMS delay spread of 370 ns and 4000 ns respectively as outlined in Table 4-4. For both models, a maximum Doppler of 70 Hz was used, as given in [5]. In relation to the carrier frequency of about 5.9 GHz in the considered spectrum, this corresponds to a very low speed mobility model, where no degrading impact from Doppler is expected.
.

Table 4-4: Delay Profile for ITU Vehicular Channels

Channel A		Channel B	
Excess tap delay (ns)	Relative power (dB)	Excess tap delay (ns)	Relative power (dB)
0	0.0	0	-2.5
310	-1.0	300	0
710	-9.0	8900	-12.8
1090	-10.0	12900	-10.0
1730	-15.0	17100	-25.2
2510	-20.0	20000	-16.0

The Channel A model was extended to also support higher bandwidths. Table 4-5 shows the Extended Vehicular A (EVA) model.

Table 4-5: Delay Profile for EVA Channel

Excess tap delay (ns)	Relative power (dB)
0	0.0
30	-1.5
150	-1.4
310	-3.6
370	-0.6
710	-9.1
1090	-7.0
1730	-12.0
2510	-16.9

Figure 4-10, Figure 4-11 and Figure 4-12 show the BLER performance comparison between C-V2X and ITS-G5 for ITU-VA, VB and EVA models respectively. In general, the following conclusions can be made.

1. It can be seen that for all the considered channel models, C-V2X exhibits a gain ranging between 1 to 4 dB with the exception of 16QAM ¾ where both the technologies exhibit similar performance.
2. At SNRs > 15 dB, ITS-G5 shows a flattening effect. This is due to the packet being not detected and hence considered as a packet loss. C-V2X does not show such flattening behaviour.
3. Both technologies perform very poorly for ITU-VB. This is due to the very large delay spread (20000 ns) that is way greater than the CP length and thereby causing high inter-symbol interference. However, it can be noted that C-V2X still performs superior than ITS-G5.
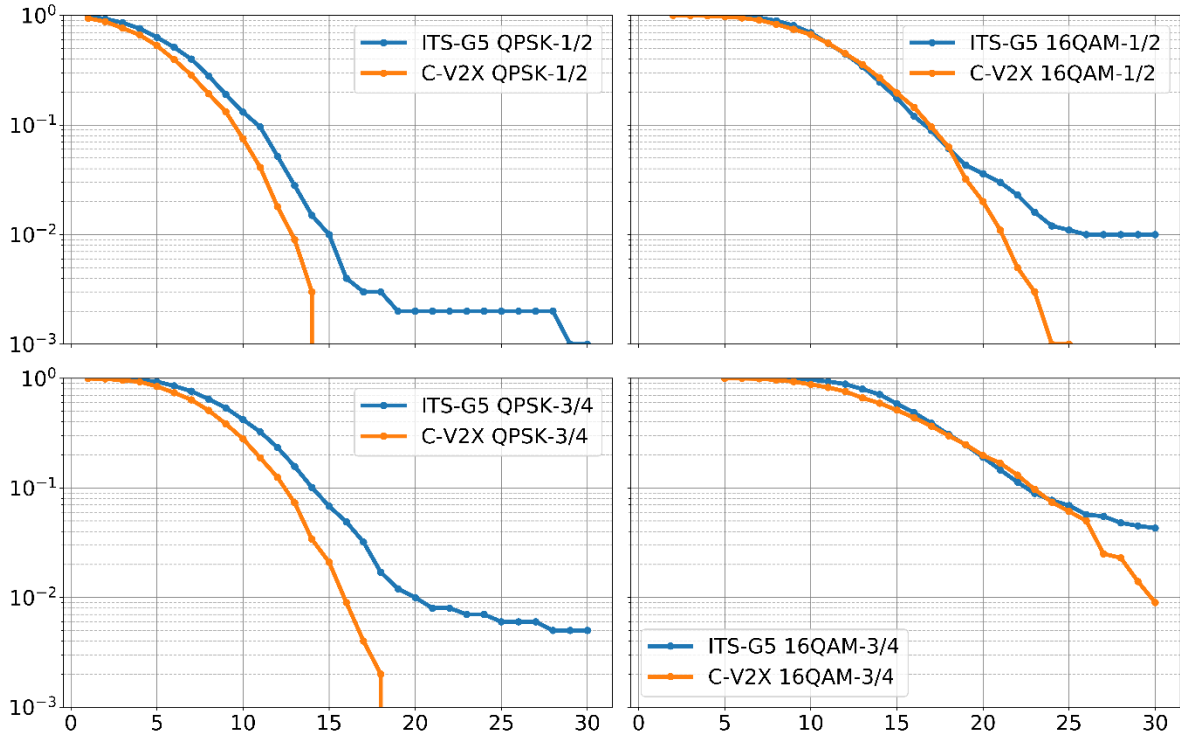
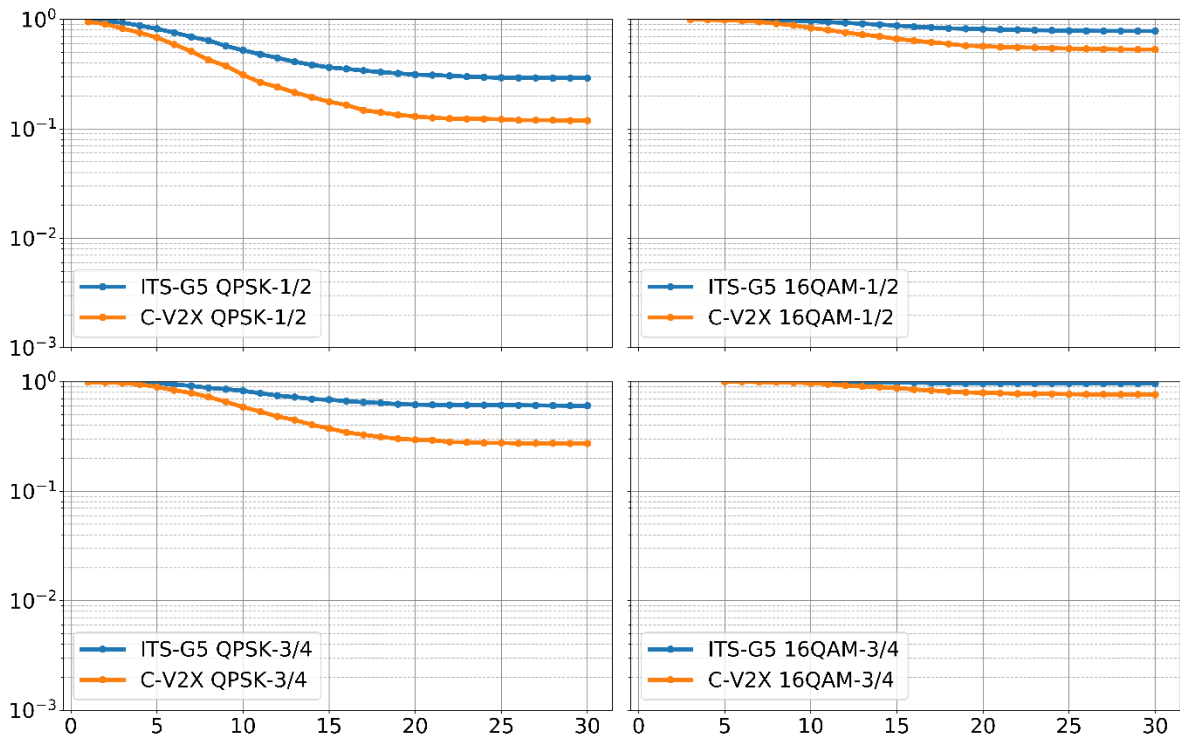*Figure 4-10: BLER vs. SNR (dB) for ITU Vehicular A*

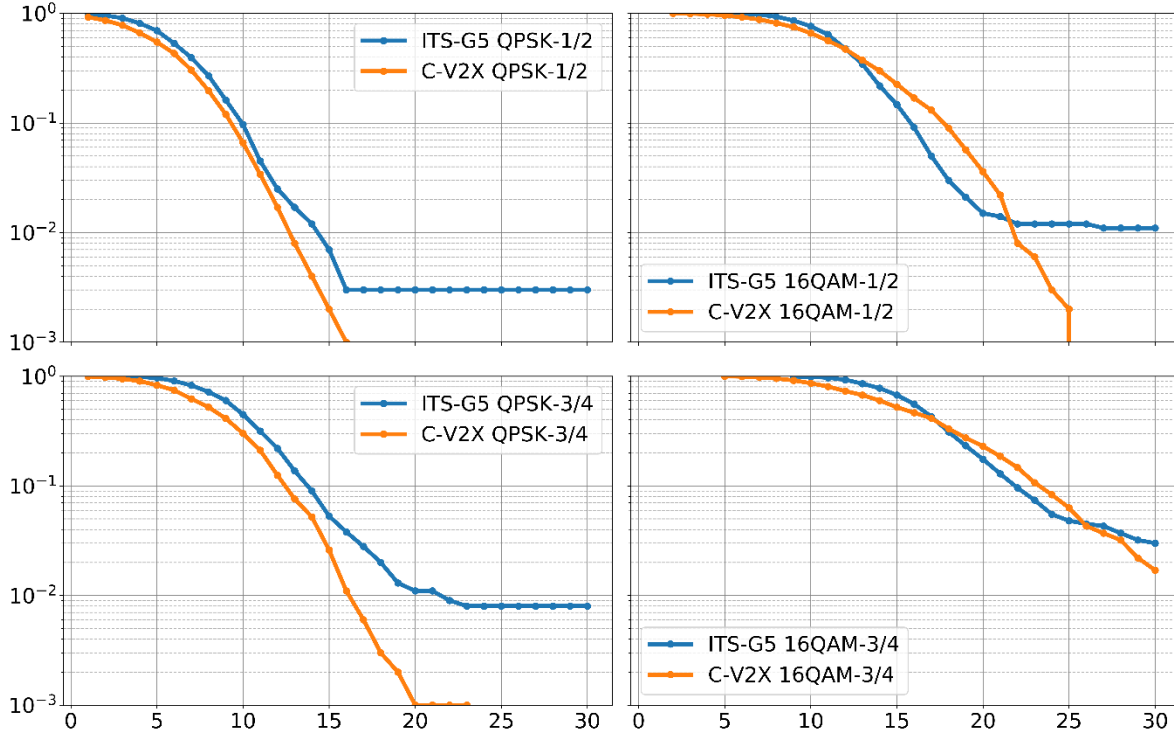*Figure 4-11: BLER vs. SNR (dB) ITU Vehicular B*

Figure 4-12: BLER vs. SNR (dB) ITU Extended Vehicular A

4.3.2.2 ITU Channel Models - SIMO Channels

The ITU channels models (VA, VB and EVA) also support multiple antennae by means of specifying the MIMO correlation matrices. Here, we consider a 1X2 configuration with 1 transmit and 2 receive antennas with the correlation matrix as defined in 3GPP TS 36.101 Table B.2.3.1-2

	One antenna	Two antennas	Four antennas
UE Correlation	$R_{UE} = 1$	$R_{UE} = \begin{pmatrix} 1 & \beta \\ \beta^* & 1 \end{pmatrix}$	$R_{UE} = \begin{pmatrix} 1 & \beta^{1/9} & \beta^{4/9} & \beta \\ \beta^{1/9^*} & 1 & \beta^{1/9} & \beta^{4/9} \\ \beta^{4/9^*} & \beta^{1/9^*} & 1 & \beta^{1/9} \\ \beta^* & \beta^{4/9^*} & \beta^{1/9^*} & 1 \end{pmatrix}$

The values for α and β depend on the correlation type and are defined in TS 36.101 Table B.2.3.2-1

Correlation Model	α	β
Low correlation	0	0
Medium Correlation	0.3	0.9
Medium Correlation A	0.3	0.3874
High Correlation	0.9	0.9

Hence, for our considered configuration of 1X2 with low SIMO correlation, the Tx correlation matrix is 1 and the Rx correlation matrix is a 2X2 identity matrix.
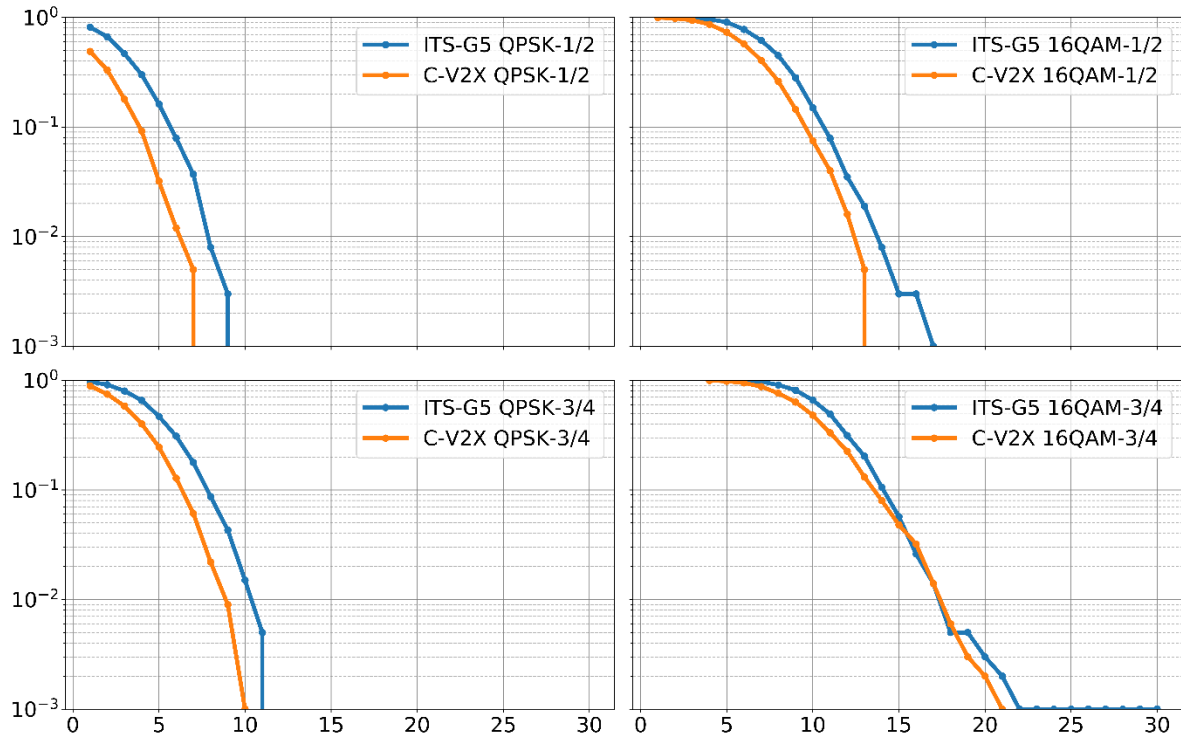
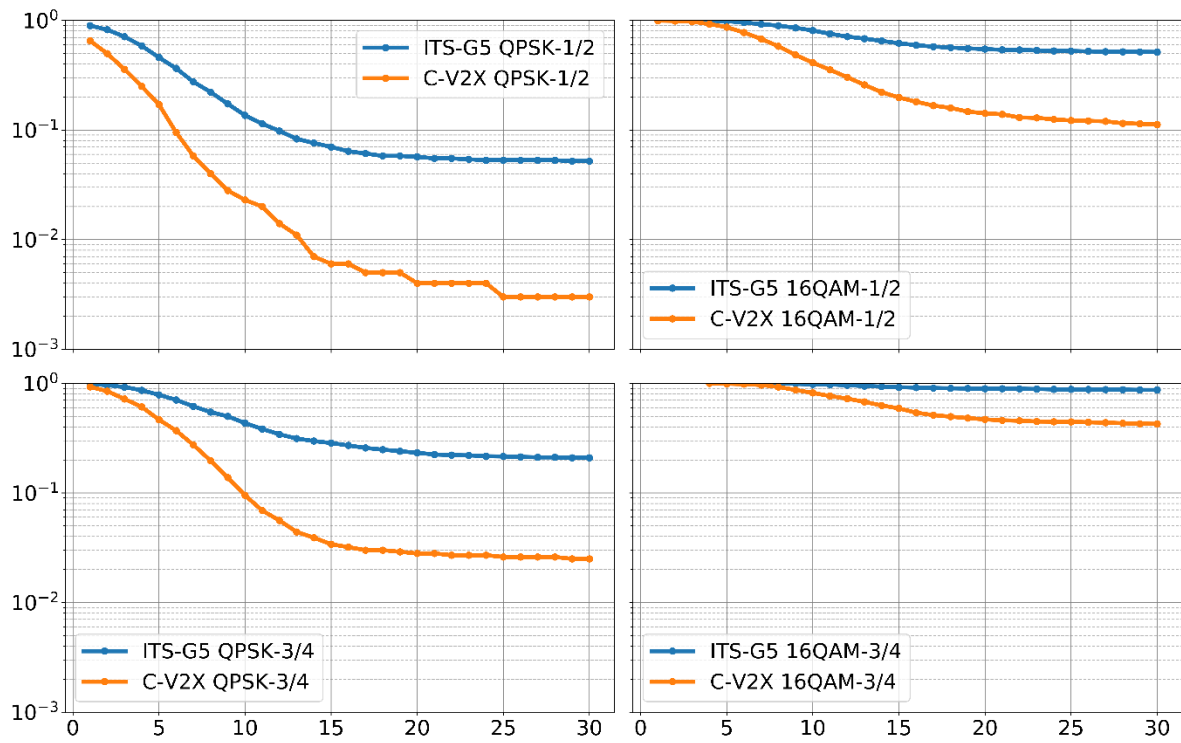*Figure 4-13: BLER vs. SNR (dB) ITU Vehicular A (SIMO)*

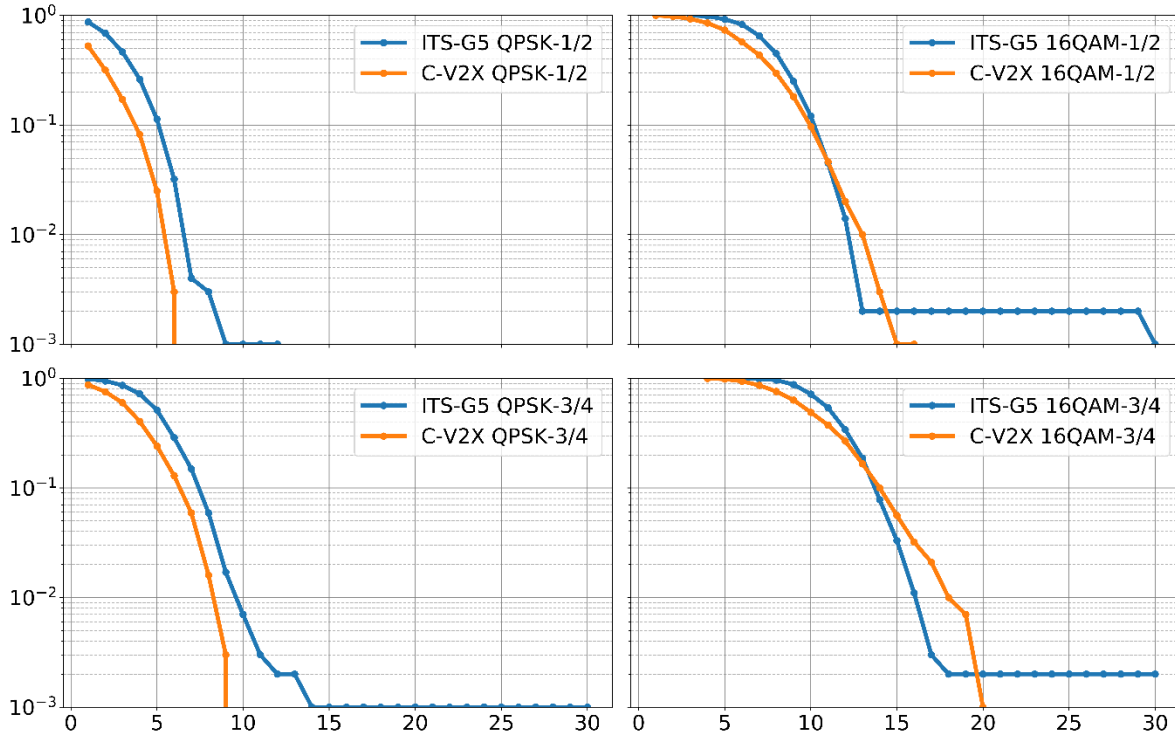*Figure 4-14: BLER vs. SNR (dB) ITU Vehicular B (SIMO)*

Figure 4-15: BLER vs. SNR (dB) ITU Extended Vehicular A (SIMO)

Figure 4-13, Figure 4-14 and Figure 4-15 shows the BLER performance of C-V2X and ITS-G5 for ITU MIMO channels. It can be seen that due to 2 receiving antennas, the performance has been significantly improved. For the SIMO channel models, the QPSK schemes in C-V2X perform better over their ITS-G5 counterparts exhibiting a gain of 1 - 3 dB. The 16QAM schemes of C-V2X perform on par or better than ITS-G5 for the ITU-VA channel model. For the case of ITU-EVA, the 16QAM schemes for C-V2X perform better over ITS-G5 at low SNRs whereas ITS-G5 marginally outperforms C-V2X at higher SNR's. However, this behaviour is compensated by the flattening effect exhibited by ITS-G5.

Both schemes show performance gain for ITU-VB channel. However, here C-V2X seems to be the clear winner with both the QPSK schemes outperforming those of ITS-G5 by at least an order of magnitude (at SNR of 13 dB, the BLER of C-V2X QPSK ½ is 1e-2 whereas for ITS-G5 it is only 1e-1). However, the 16QAM schemes still do not show any significant performance enhancement over the SISO case.

4.3.2.3 C-ITS Field Trails in Australia, Europe and US

During the years 2007 to 2010, a total of 35 field trial campaigns were conducted on public roads in US, Germany, Austria, Italy and Australia totalling over 1100 km [6]. These campaigns demonstrated different V2I and V2V use cases such as IMA, DNPW, EEBL and driving along roads equipped with RSUs. For each test location, multiple repetitions of a scenario were run transmitting BSMs at an aggregate of 400 packets/s. For the purpose of measurement, vehicles mounted with a Cohda Wireless MKI 802.11p DSRC unit with single antenna were used. The channel sounding data captured during the field trials were analysed to obtain delay and Doppler spread characteristics.

Table 4-4-4: Delay and Doppler Spread characteristics [4]

	Delay Spread (ns)				Doppler Spread (Hz)			
	RMS		Maximum		RMS		Maximum	
QUANTILE	50%	90%	50%	90%	50%	90%	50%	90%
URBAN LOS	34.8	81.6	362.0	756.6	40.0	108.3	353.4	665.0
URBAN NLOS	65.4	124.7	468.9	848.4	63.1	140.9	360.7	814.2
HIGHWAY LOS	18.7	61.7	272.3	744.0	59.7	169.8	826.1	1361.6
HIGHWAY NLOS	58.8	131.3	509.7	971.9	154.9	322.4	875.2	1446.5

Using these statistics, a total of 6 channel models were proposed for different scenarios and were also accepted as standard models for 5.9 GHz V2V [5]. They are outlined below.

Table 4-4-5: Models with Delay Profiles

Scenario	Path Delays (ns)	Path Gains (dB)	Doppler Shift [Hz]	Doppler Type
Rural LOS	[0, 83, 183]	[0, -14, -17]	[0, 492, -295]	Static, Half-BT
Urban Approaching LOS	[0, 117, 183, 333]	[0, -8, -10, -15]	[0, 236, -157, 492]	Static, Half-BT
Urban NLOS	[0, 267, 400, 533]	[0, -3, -5, -10]	[0, 295, -98, 591]	Static, Half-BT
Highway LOS	[0, 100, 167, 500]	[0, -10, -15, -20]	[0, 689, -492, 886]	Static, Half-BT
Highway NLOS	[0, 200, 433, 700]	[0, -2, -5, -7]	[0, 689, -492, 886]	Static, Half-BT

The first path of all the models (associated with delay 0 and a gain 0) is assumed to be static LOS with a Rician fading distribution. The remaining paths are assumed to be pure Rayleigh with a half-bathtub (Half-BT) Doppler spectral shape.

Figure 4-16, Figure 4-17, Figure 4-18, Figure 4-19 and Figure 4-20 show the BLER comparison between C-V2X and ITS-G5 for the scenarios mentioned in Table 4-4-5. The following conclusions can be made

1. For the rural LOS scenario where other vehicles and buildings are absent, the path delays and the associated Doppler shifts are quite low and the CP length is more than enough to compensate for these delays. Hence, both the technologies show a BLER of 10e-3 at SNR < 10 dB. C-V2X shows a gain of 1 - 2 dB over ITS-G5 for both the QPSK schemes. However, this gain is not so profound for 16QAM ½.

2. For urban approaching LOS where two vehicles approach each other in an urban setting with buildings nearly, the performance of both the technologies is almost identical for QPSK ½ scheme. For QPSK ¾ and 16QAM schemes, C-V2X exhibits better performance at lower SNRs but shows lower descent in BLER as the SNR increases when compared to ITS-G5. This can be due to the higher packet sizes used in C-V2X compared to the ones used on ITS-G5. However, the performance converges at very high values of SNRs.

3. The QPSK performance of C-V2X for urban NLOS scenario is apparently better than ITS-G5 with a gain ranging from 0 - 3 dB. In the case of 16QAM ½, both technologies exhibit same

performance over lower SNR region and at SNR >15, the C-V2X shows higher slope whereas ITS-G5 flattens out. In contrast, the 16QAM ¾ performance of ITS-G5 is better than C-V2X in the sense that ITS-G5 shows a higher descent in BLER at mid SNR range, but the performance converges at high SNR values.

4. The performance of both technologies is almost identical for highway LOS scenario with C-V2X showing a slightly better performance except in the case of 16QAM ¾ where ITS-G5 shows a higher descent in BLER as the SNR increases.

5. For highway NLOS, C-V2X QPSK schemes have a significant gain over ITS-G5 in the range of 0 - 5 dB whereas the performance is the same for 16QAM ½ with C-V2X showing a steeper descent as the SNR increases. The performance over 16QAM ¾ worsens for both the technologies and follows the same trend as previous models.
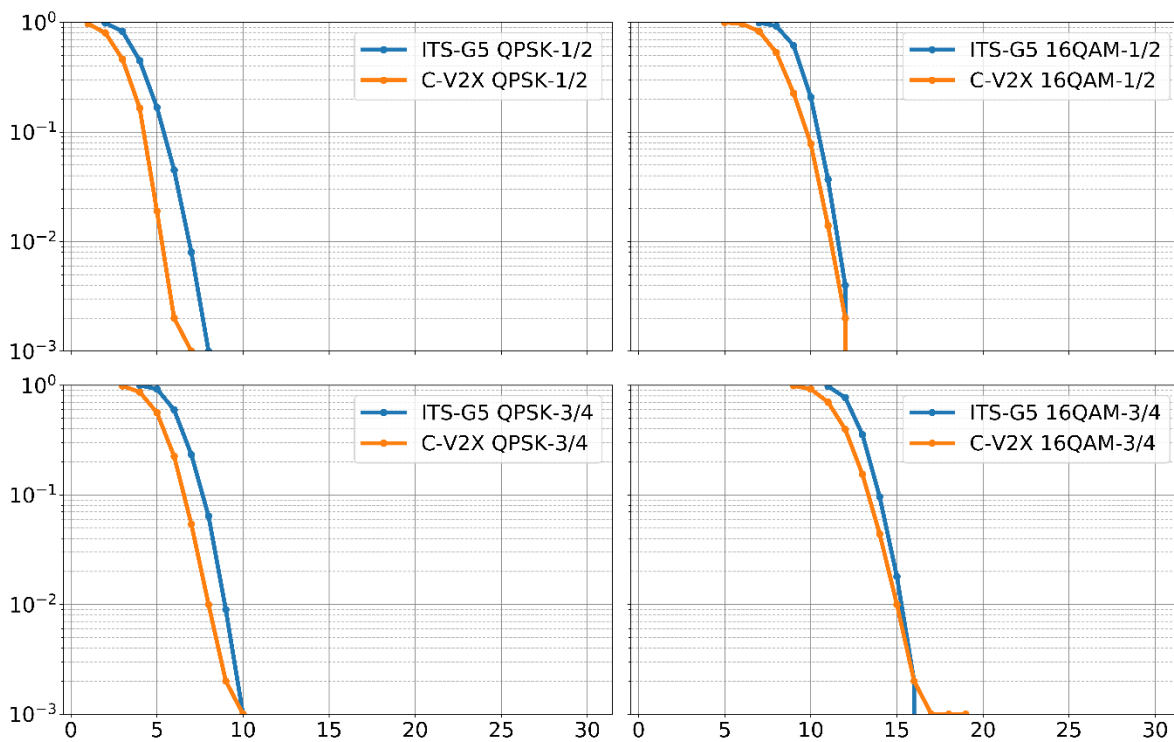

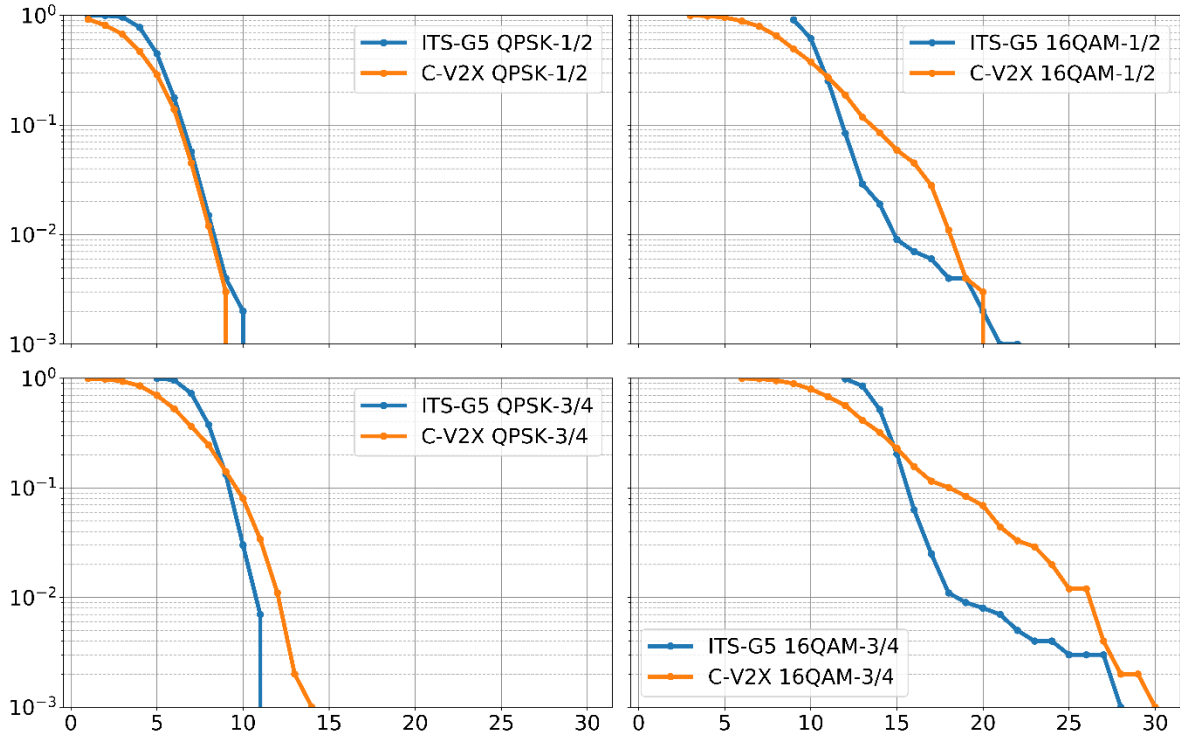*Figure 4-16: BLER vs. SNR (dB) Rural LOS Scenario*

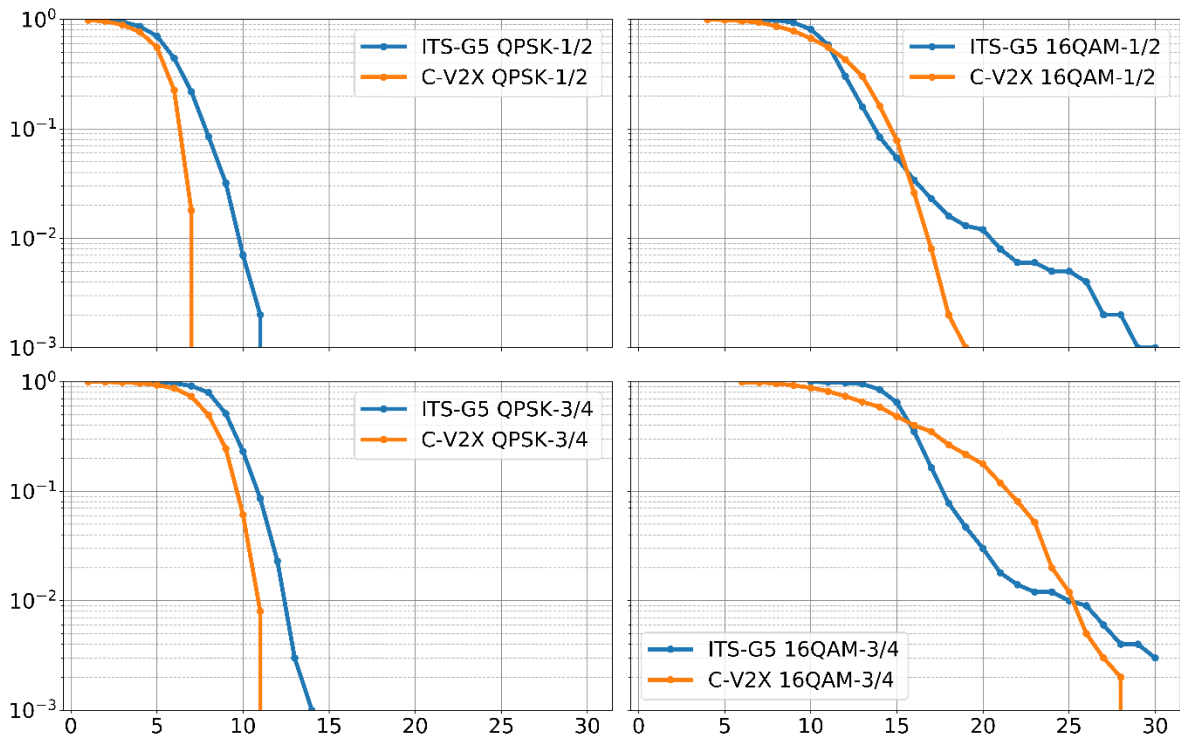*Figure 4-17: BLER vs. SNR (dB) Urban Approaching LOS Scenario*

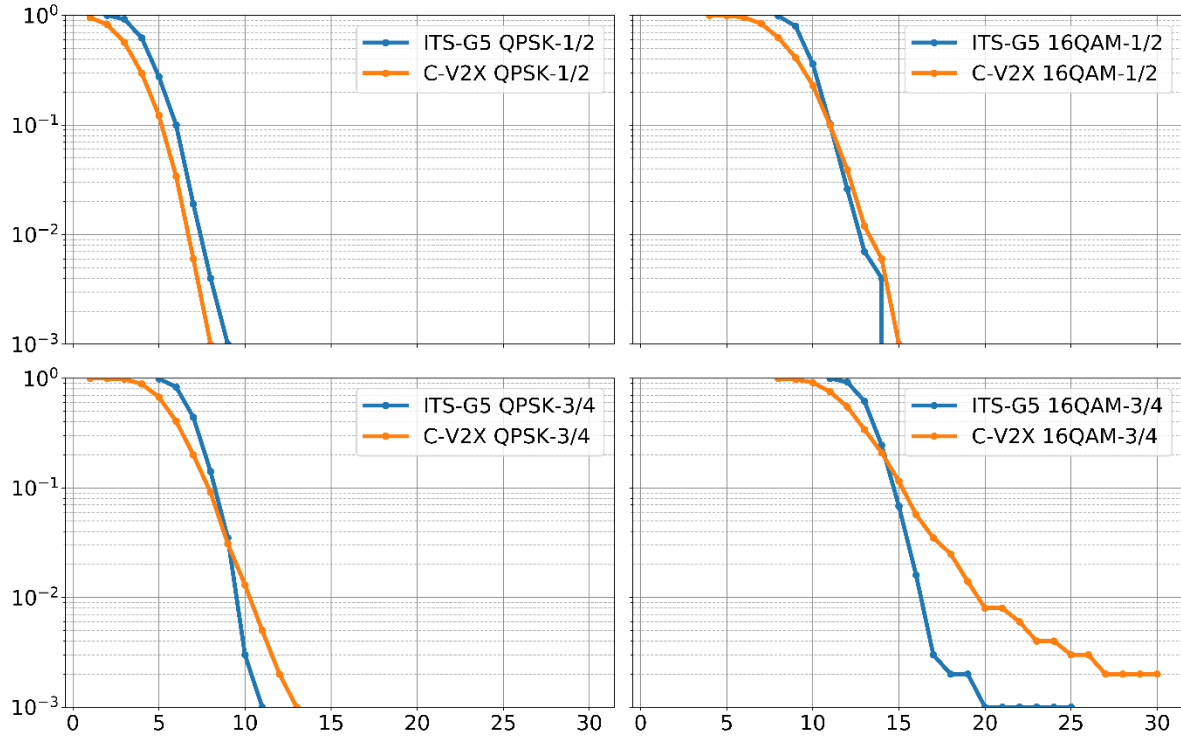*Figure 4-18: BLER vs. SNR (dB) Urban NLOS Scenario*

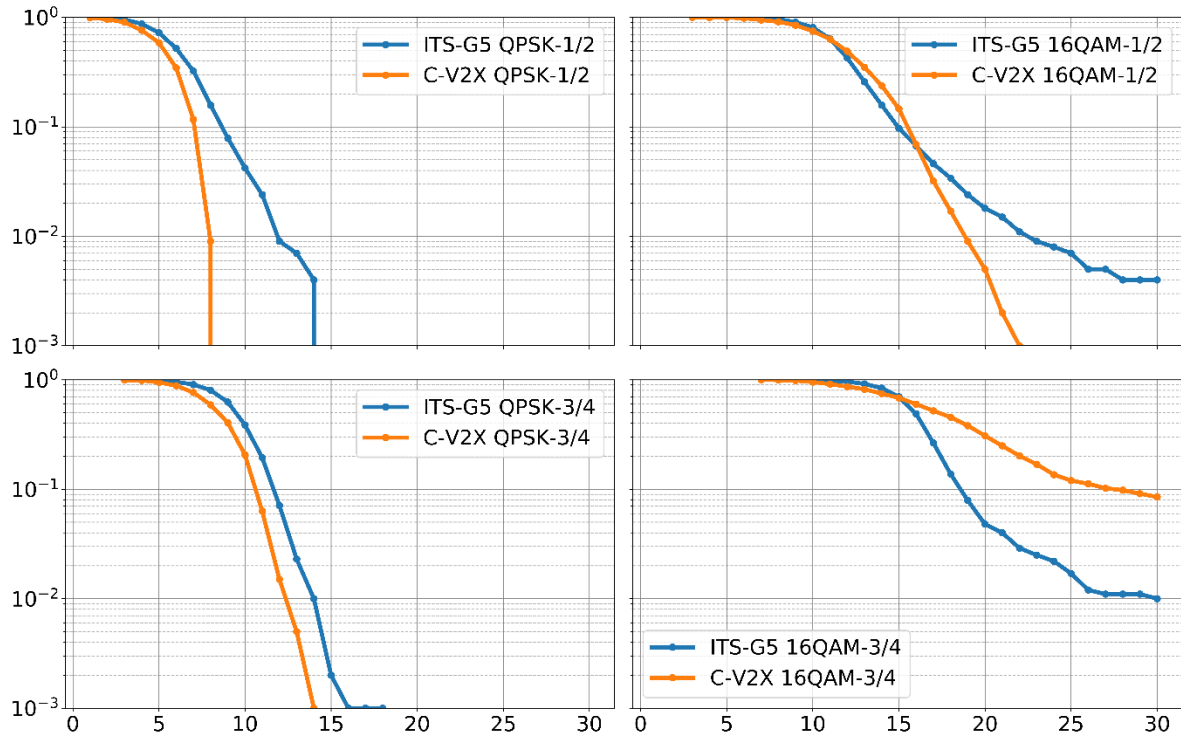*Figure 4-19: BLER vs. SNR (dB) Highway LOS Scenario*

Figure 4-20: BLER vs. SNR (dB) Highway NLOS Scenario

4.4 C-V2X Specific Results

In this section, the performance analysis of C-V2X for various reference channel models is presented.

4.4.1 Reference Channel performance for Calibration

The purpose of this analysis is to verify the PSSCH demodulation performance with a single active link and see that it conforms to the performance specification. The performance requirements are outlined in Table 4-6 and are taken from Table 14.2-1 of TS 36.101.

Table 4-6: Test Parameters

Test num.	Bandwidth	PSSCH Reference channel	Propagation condition	Reference value	
				PSSCH BLER (%)	SNR (dB) of PSSCH
1	20 MHz	CD.8	EVA180	10	14.2
2	10 MHz	CD.9	EVA2700		5.4

Where the configurations CD.8 and CD.9 given in TS 36.101 Annex A.8.5 and are shown below.

Table 4-7: Reference Channels

Parameter	Unit	Value		
Reference channel		CD.8	CD.9	CD.10
Channel bandwidth	MHz	20	10	20
Allocated resource blocks		8	3	3
DFT-OFDM Symbols per subframe (see Note 1)		9	9	9
Modulation		16QAM	QPSK	QPSK
Transport Block Size		1800	208	504
Transport block CRC	Bits	24	24	24
Number of PSSCH transmissions		1	2	1
Binary Channel Bits (see Note 2)	Bits	3456	648	648
Note 1: PSSCH transmissions are rate-matched for 10 DFT-OFDM symbols per subframe, and the last symbol shall be punctured as per TS 36.211. Note 2: Binary Channel Bits are calculated under assumption of 9 symbols. Note 3: If more than one Code Block is present, an additional CRC sequence of L = 24 Bits is attached to each Code Block (otherwise L = 0 Bit).				

Figure 4-21 shows the BLER performance for the reference parameters CD.8 and CD.9 as outlined in Table 4-7. It can be seen for the case of CD.8, the simulation perfectly matches the standard specification. However, for the case of CD.9 with a high Doppler, there is an offset of almost 1.5 dB. This behaviour may be due to the channel modelling imperfections used in the simulation. At high Doppler values, the simulation seems to produce unexpected results.
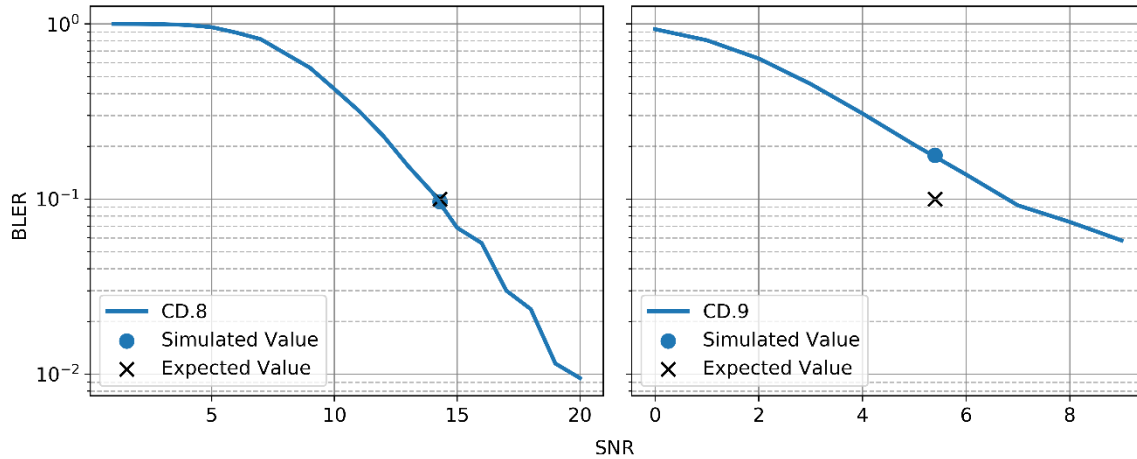
Figure 4-21: BLER vs. SNR in dB Performance for Reference Channels CD.8 and CD.9

4.4.2 Effect of Retransmissions

C-V2X supports one blind retransmission by default within any given sidelink period. The receiver maintains a HARQ buffer with the scheduled sidelink transmissions and soft combines (adding the soft bits) both the transmission instances in order to decode the received message. In order for this to work, the receiver needs to know exactly the subframe in which the retransmission will be scheduled. This information is embedded in the SCI message in the first transmission instance by means of a parameter known as *timegap* which specified the gap (in subframes) between the first and the subsequent retransmission. Once the receiver decodes the first SCI message, it knows this timegap. It proceeds with decoding the data message. If the data message decoding is not successful, it puts the current soft bits into a buffer and combines them with the retransmission that occurs after the timegap. If the first decoding attempt is already successful, the receiver has the option to either discard the retransmission or combine them again in order to increase the reliability of the decoded message.

In this analysis, the performance of C-V2X for different speeds is illustrated with and without the use of retransmissions. The underlying channel model is assumed to be ITU-EVA. The MCS scheme is assumed to be QPSK 1/3 which is the reference configuration as defined in TS 36.101 Table A.8.3-1. This corresponds to a packet size of 3496 bits with an MCS scheme 4. Simulations have also been carried out for all other MCS schemes. For the purpose of illustration, only QPSK 1/3 is shown here. The remaining MCS schemes are outlined in Appendix A.1

Figure 4-22 and Figure 4-23 outline the BLER performance of C-V2X for the case of no retransmission and 1 blind retransmission respectively. It can be seen that with 1 blind retransmission, there is an additional gain of 4 - 6 dB. The gain is also more pronounced for higher speeds where the case of no retransmissions exhibits flattening. The results show that 1 blind retransmission can significantly increase the system performance especially at higher speeds. However, for the case of 500 km/h, the retransmissions would still result in flattening of the performance. This may be due to the high Doppler (~2733 Hz) associated with such high speed.

Since, the data message can only be decoded if the control message is decoded, it is important that the SCI message can be decoded even at very low SNR's. As seen from Figure 4-24, the SCI message is decoded even at very low SNR's and also for high speeds. It can be noted that due to the use of

convolutional encoder, the curves show lesser slope than data transmissions. However, the better performance of the control channel is due to the high coding gain used for SCI message (SCI message is 48 bits with 16CRC which is spread to 480 bits after convolutional encoding and rate matching) and this corresponds to 240 QPSK symbols spanning over 2 PRBs. This big spreading is the reason for good performance of control channel even at high speeds.

NOTE: In real systems, the transmit power of the control message is boosted by an additional 3dB. This makes the control channel messages decodable for even lower SNR. This performance can be visualized by simply shifting the SNR points (by 3 points) to the left in Figure 4-24.
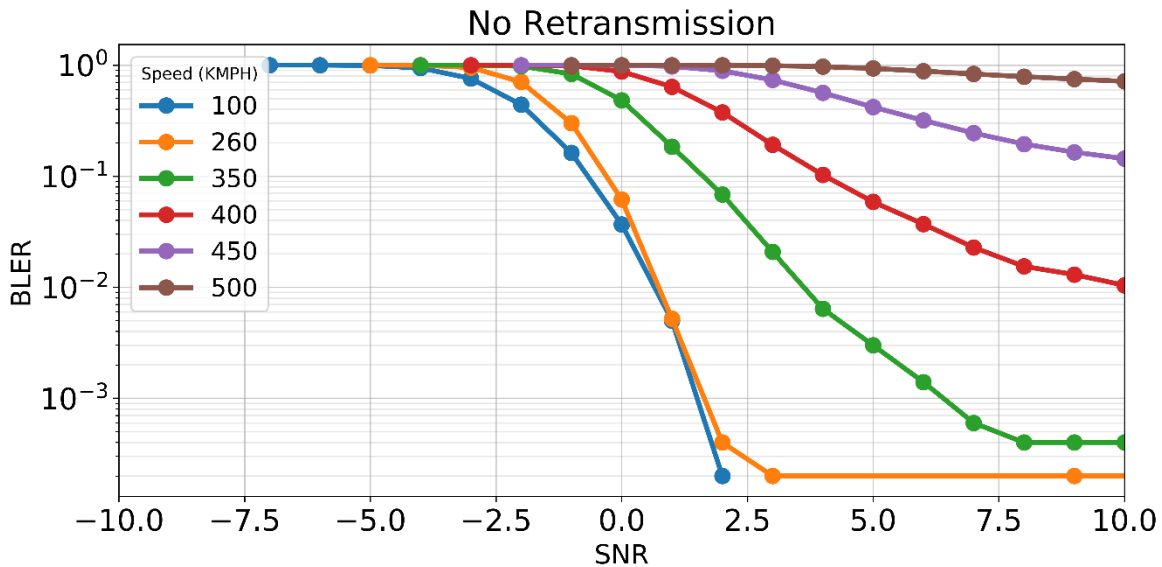

Figure 4-22: C-V2X BLER vs. SNR in dB Performance for different speeds without retransmission
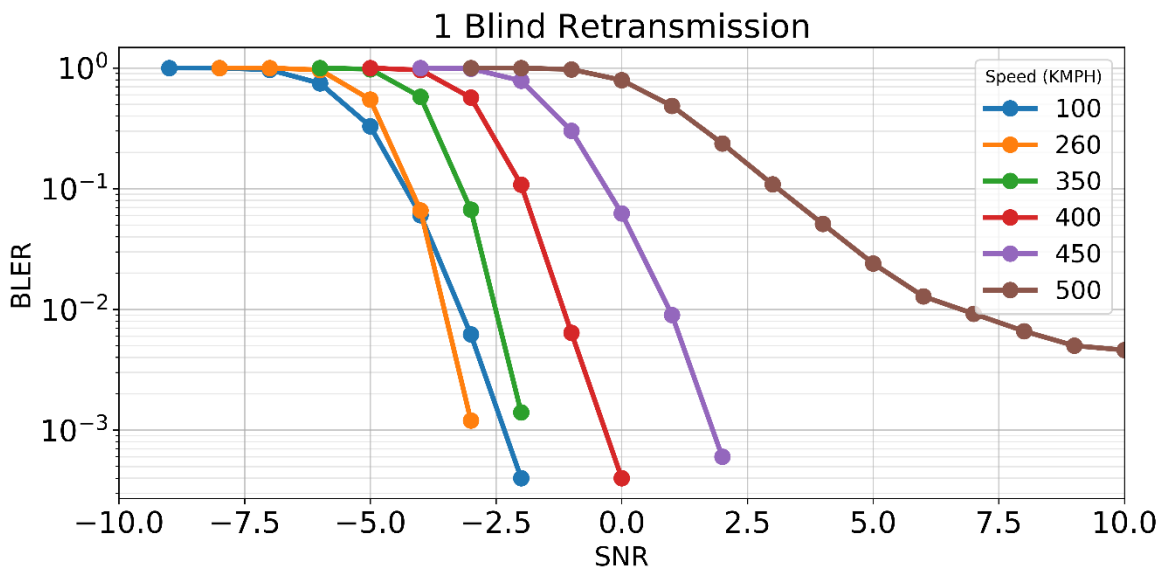

Figure 4-23: C-V2X BLER vs. SNR in dB Performance for different speeds with retransmission
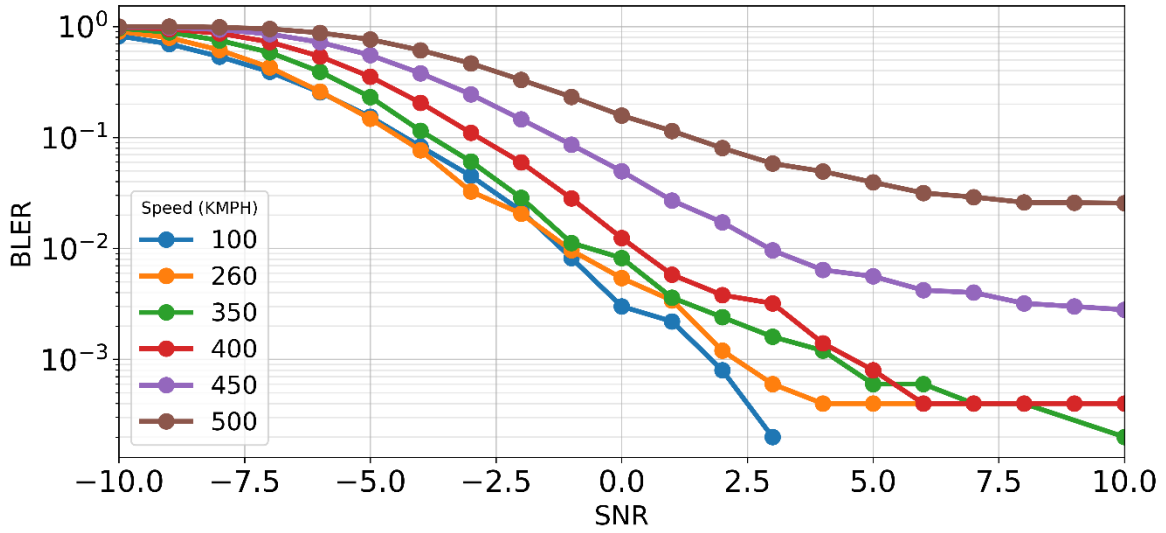
Figure 4-24: BLER vs. SNR in dB performance of SCI message

5 System Level Simulation Results

5.1 System description

Direct C-V2X communication through sidelink is a mode of communication whereby a User Equipment (UE) can directly communicate with other UEs in its proximity over the PC5 air interface. This communication is a point-to-multipoint communication where several receiving UEs (Rxs) try to receive the same data packets transmitted from a transmitting UE. In the present section, we discuss system level simulation results obtained for network-assisted direct C-V2X transmission in a highway traffic scenario, as illustrated in Figure 5-1. All UEs are connected to eNBs of the same RAN. Scheduling and resource control information is transmitted from eNBs to the UEs via the V2N C-plane of the radio interface. The transmitting UE (Tx) directly transmits its V2V/V2I sidelink data packets to the surrounding Rxs with its communication range, thereby achieving low latency.

The RAN can provide network control for the direct C-V2X communication. In 3GPP-defined C-V2X, there are two alternative sidelink transmission modes:

- Sidelink transmission mode 3
  In this mode, the resource allocation for each sidelink transmission is scheduled by an eNB. This transmission mode is only available when the vehicles are under cellular coverage. To assist the resource allocation procedure at the eNB, UE context information (e.g., traffic pattern information) can be reported to eNBs.

- Sidelink transmission mode 4
  In this mode, a Tx in C-V2X communication can autonomously select a radio resource from a resource pool which is either configured by network or pre-configured in the user device for its direct C-V2X communication over PC5 interface. In contrast to mode 3, transmission mode 4 can operate without cellular coverage.

In the system-level simulation analysis described below, transmission mode 3 is utilized for the direct C-V2X communication through sidelink which means all UEs are under the coverage of a cellular network which controls the resource allocation of sidelink transmissions.

The field trials performed by the ConVeX project have used mode 4. However, capacity evaluation was not part of the field trials. For the evaluation by system simulation, we have chosen mode 3, in order to also include an evaluation of this mode in the project.
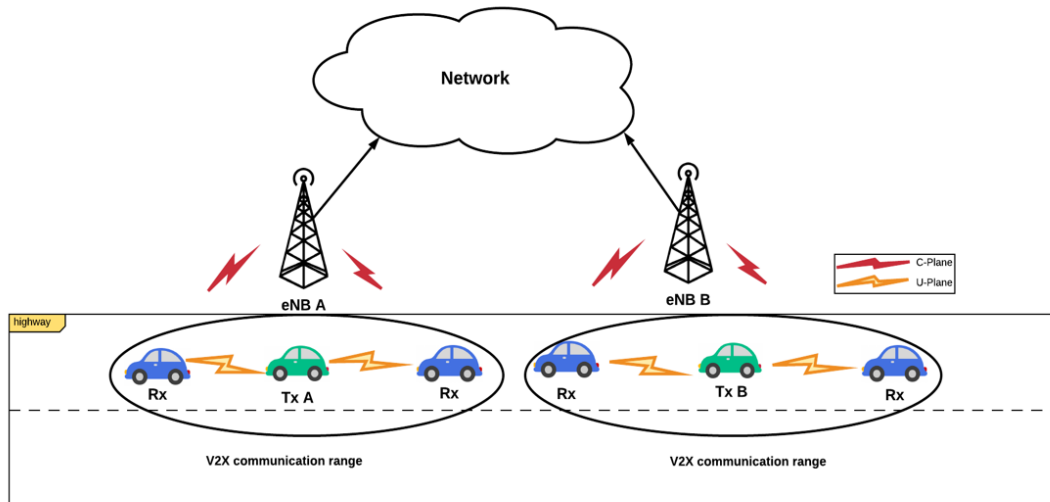
Figure 5-1: Direct C-V2X communication with network assistance on a highway

5.2 Sidelink system-level simulator

System-level simulations are generally based on multi-cell and multi-user scenarios., taking into account the system relevant functionalities like network layout, channel model, scheduling and characteristics of eNBs and a mobile UEs. However, for system-level simulation of the sidelink C-V2X communication, data packets are directly transmitted from a Tx UE to the Rx UEs without going through the eNBs. eNBs are only responsible for providing the resource allocation to UEs under coverage. As Figure 5-1 shows, in the first evaluated scenario the Tx and all Rxs in its communication range are covered by the same eNB. Hence, the Txs have a constrained location range which can make sure that all Rxs that are in this Tx's communication range are covered by the same eNB. The interference is from the UEs who are utilizing the same transmission resource and transmitting data packets simultaneously but are covered by the adjacent eNB. Such a simplified scenario helps us to understand the effects of inter-cell interference.

A more realistic scenario is also considered where the Tx is served by the eNB to which it has a better link. This is in contrast to the previous case where the Tx is always associated to the closest eNB. This assumption leads to cases where the transmitting UE and the interfering UE are in the same geometrical cell area and hence gives rise to increased intra-cell interference. This is illustrated in Figure 5-2 and Figure 5-3 where we show a UE deployment example where UEs are not necessarily constrained to be in the geometric coverage area of a single eNB. It can be noted that Rx1 and Rx2 are well into the geometric cell area of eNB A which also happens to be where an interfering Tx A is located. Hence, these receivers experience a higher interference. Additionally, it is also possible for the Tx to be located in eNB A's geometric cell area but serviced by eNB B due to a better link. One reason for this is high shadowing for the eNB A link. In this case, both the transmitting UE and the receiving UE are geographically in the same cell resulting in very high intra-cell interference and subsequently a lower PRR.
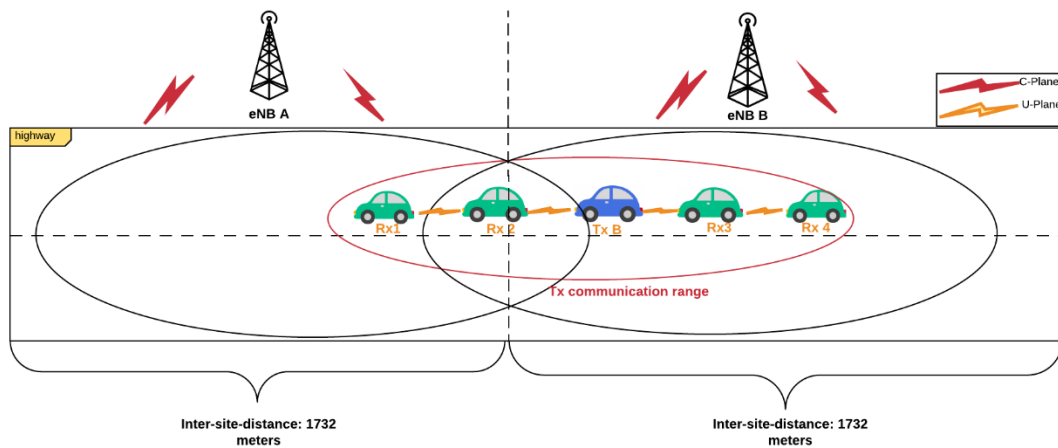
Figure 5-2: C-V2X UE deployment example where UEs are not necessarily controlled by closest eNB due to pathloss based handover, example I
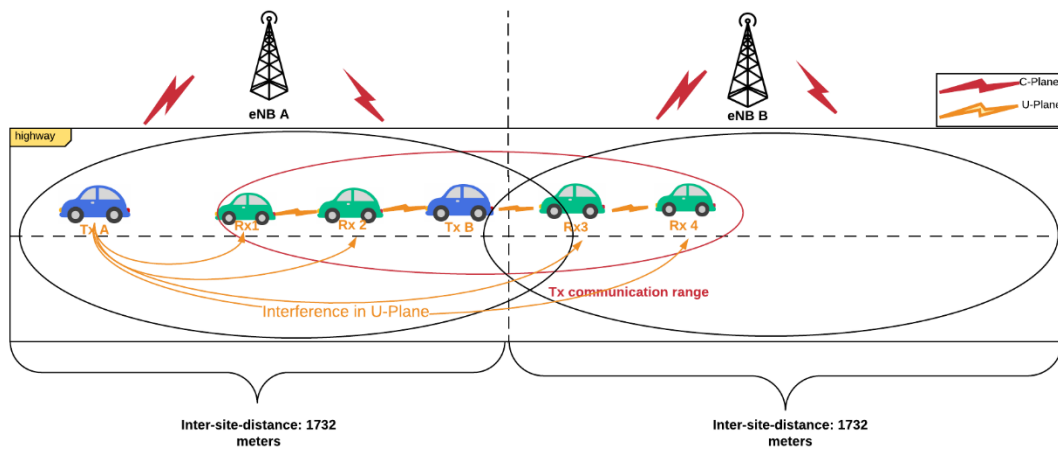

Figure 5-3: C-V2X UE deployment example where UEs are not necessarily controlled by closest eNB due to pathloss based handover, example II

Moreover, the system level simulation mainly reflects the Media Access Control (MAC) layer functionalities such as resource allocation, user scheduling, and adaptive modulation and coding scheme, rather than the physical layer processing. The performance of the physical link is taken into account by a Link-to-System (L2S) interface derived from link level simulations. Moreover, to precisely reflect the characteristics of a radio link (e.g., frequency fading), a L2S mapping needs to be accurately formulated. Mutual information based L2S is one of the commonly used methods which has been considered as preferable and applicable. Physical-layer procedures have to be abstracted by accurate but also low-complexity models.

For our system level simulations, we used the following L2S mapping tables:

1. The AWGN mapping table for all MCS (0 - 20) as shown in Figure 4-8. This mapping table considers no fading nor retransmissions. This mapping is denoted L2S-1.

2. The mapping table that considers all MCS (0 - 20) for the EVA fading channel at different speeds. No blind retransmission is considered. This mapping is denoted L2S-2 and respective curves are given in Appendix A, Figure A-1 to Figure A-6.
3. The mapping table that considers the same channel and speeds as L2S-2 but with one blind retransmissionFigure 4-23. This mapping is denoted L2S-3 and respective curves can be found in Appendix A, Figure A-7 to Figure A-12.

In our system-level simulation, resource allocation, mobility management, admission control, interference management, hybrid automatic repeat request (HARQ), and scheduling are modelled. The Key Performance Indicators (KPIs) are Signal-to-Noise-plus–Interference-Ratio (SINR), MCS, , BLER, and the Packet Reception Ratio (PRR). We consider the traffic consists of CAM messages, where each message is contained in a single packet, which in turn is contained in a single transport block. For this reason, the PRR is simply the inverse of the BLER.

The PRR is calculated from all Rxs within the intended communication range of the Tx. For each transmitted CAM message, the PRR can be calculated as X/Y, where Y is the total number of UEs located in the communication range from the UE transmitting the message, and X is the number of UEs in that range that successfully receives the message [1]. The average PRR is calculated as:

$$\frac{X_1 + X_2 + \cdots + X_n}{Y_1 + Y_2 + \cdots + Y_n}$$

(5-1)

where the index represents the message for which the reception is evaluated and n is the total number of messages in the simulation. When a UE is transmitting, i.e. is in the role of a Tx UE, in practice it cannot receive at the same time. Since multiple packets may be transmitted by other Tx UEs at the same time, on different frequency resources, a UE may miss multiple packets while it is itself transmitting. The missed packets due to this restriction are, however, not reflected in the PRR in the system simulator.

5.2.1 Sidelink system-level simulation assumptions

In this section, we highlight in detail the simulation assumptions.

5.2.1.1 Environment Model

Two eNBs are deployed with an Inter-Site-Distance (ISD) of 1732 meters alongside the 3464-meter highway scenario with 6 lanes to provide control for the UEs of the C-V2X communication. The 2 eNBs are centered along the highway, i.e. the eNBs are placed at +/-1732m/2 from the horizontal center of the highway.

Due to the limited number of cells and due to our methodology in the first scenarios where we only consider the UEs that are in-between the 2 eNBs, the interference in the simulated scenario will be substantially smaller than in practice and the results are therefore optimistic. In one simulation scenario the highway length is extended to 6928-meter, with 4 eNBs deployed, so that the edge area in which interference is reduced represents a rather small fraction of the total area.

UEs are deployed with a fixed Inter-Vehicle-Distance (IVD) on each lane in the beginning of the simulation. During the simulation no UEs are entering or leaving. We assume the desired communication range of the UEs is 400 meters [2]. Results are presented in the range of ISD = 5 to

100 meters independent of vehicle speed. Note that in realistic traffic scenarios IVD in meters is typically equal or larger than half the vehicle speed measured in kilometers per hour, e.g. IVD ≥ 50 m at speed of 100 km/h.

The number of UEs on the highway scenario has been calculated as:

$$\text{UE}_H = \frac{L_H}{IVD} * Lane$$

Where L_H is the length of the highway scenario, $Lane$ is the number of highway lanes, and IVD is the inter vehicle distance.

5.2.1.2 Traffic model

The number of the UEs controlled by each eNB is calculated as:

$$\text{UE}_{eNB} = \frac{ISD}{IVD} * Lane$$

Where ISD is the ISD and IVD and $Lane$ are defined as in the equation before.

We assume each UE transmits a packet of 256 bytes 10 times per second on average in most scenarios. The packet transmission rate is a variable parameter in some of the results we will show further below.

The data volume (in bits per second) is derived as follows:

$$C = ps * 8 * UE_{eNB} * P$$

where ps is the packet size of 256 byte, $P = 10$ is the average number of packet transmissions per second, and UE_{eNB} is obtained from the equation before.

5.2.1.3 Resource allocation and scheduling

Direct C-V2X communication in transmission mode 3 uses resources in so-called resource pools. The resource pools are configured by the eNB to its controlled UEs. Rx UEs monitor the Physical Sidelink Control Channel (PSCCH) in the configured resource pool for transmissions from Tx UEs. The eNB precisely specifies the time-frequency resources to be used by each of its controlled Tx UEs. The Rx UEs are not informed about this by the eNB. They will get the information from the monitored PSCCHs. Typically, and in our simulation scenarios, the resource pools configured by all eNBs are the same. In this way it is ensured, that the Rx UEs can receive transmissions from Tx UEs controlled by any eNB. In particular, in our simulation there is one resource pool in each cell and that covers the entire time and frequency domain.

Each eNB ensures that it allocates each available resource to only a single one of its controlled transmitting UEs, so that for an Rx UE, interference can only emerge from Tx UEs controlled by a different eNB.

This is a conservative resource usage strategy, because in principle it may make sense for an eNB to allocate a resource to multiple Tx UEs if they are sufficiently far apart. There are, however, no standardized procedures how the eNB could know for which combination of Tx UEs that would be beneficial. Therefore, resource reuse among UEs controlled by one eNB is not considered here. Furthermore, with an intended communication range of 400 m and an ISD of 1732 m, there is little

room from a geographic perspective to have 2 Tx UEs transmit on the same resource without overlap between their communication ranges or overlap with that of a Tx UE controlled by a neighboring eNB.

Furthermore, there is the possibility for the eNB to configure a UE specific maximum transmit power that could further improve the SINR to a level that makes resource reusing within a cell beneficial. This possibility, however, has not been evaluated in this deliverable.

In the simulations, the time-frequency resource grid of LTE is not modelled explicitly. After the UE deployment, the simulation runs for 1000 iterations. In each iteration, for each of the eNBs, one of the UEs that are controlled by the eNB is selected randomly with equal probability for transmission. This represents a fully loaded system. The Rx UEs within the communication range of the selected Tx UE are then evaluated for the packet reception, regardless of by which eNB an Rx UE is controlled. If the system is overloaded, some UEs cannot be supported by eNB, and are therefore dropped. If the system is not actually fully loaded according to the IVD and message rate, then in a real system there would be iterations (subframes) where no UE controlled by one eNB does transmit, thereby the total interference generated in such iterations would be reduced. In our simulation, however, there is one Tx UE per eNB in each iteration, thereby overestimating the interference. For the practically relevant cases of a message rate of 10Hz, however, there is in fact one Tx UE per eNB in each iteration even for the highest considered IVD of 100m.

For the case of no-retransmissions, we calculate the SINR (γ_1) for each Rx-UE in the communication range for a selected Tx and look up the L2S-2 mapping for the corresponding BLER, using constant-value extrapolation for SINR values not covered by the link simulation range. A random number X is then generated from a uniform distribution [0, 1]. If $X > BLER$, then the packet is marked as received.

In case of a retransmission, γ_1 is calculated in the same way as outlined previously. Then, another interfering Tx is chosen randomly and a new SINR value (γ_2) is calculated for each Rx-UE in the communication range for the same selected Tx. Both these SINR values are averaged to get the final SINR, i.e., $\gamma_{final} = \frac{\gamma_1 + \gamma_2}{2}$ (in linear scale). The corresponding BLER is looked up from the L2S-3 table. Similar to the previous process, a random number X is then generated from a uniform distribution [0, 1]. If $X > BLER$, then the packet is marked as received.

Taking the average SINR over the first transmission and the retransmission is necessary because the L2S-3 table consider SINR values that are averaged over different SINR realizations. In the link simulation each realization represents a different fast fading channel realization, whereas in the light of a system simulation with different interferers the averaging also has to consider the differing SINR corresponding to interferer realizations.

5.2.1.4 Channel model

In this work, isotropic antennas are installed on the top of each vehicle at a height of 1.5 meters. A 1×2 antennas configuration is exploited for the direct C-V2X communication. Also, each Tx is assumed a constant EIRP of 23 dBm. According to 3GPP specifications, power control is applied where the transmit power depends on the used transmission bandwidth and the distance between the UE and the controlling eNB. The first part is not relevant in our simulation model as the full transmission bandwidth is always assumed to be used. The second part leads to a transmit power variation that is uncorrelated to the sidelink pathloss. This causes an increase in the SIR variance and

accordingly lower SINR at the lower tail of the SINR distribution, so this tends to lead to somewhat worse performance in reality than in the simulation.

The central carrier frequency is 5.9 GHz with a transmission bandwidth of 10 MHz [2]. The WINNER II models [2] are applied as propagation models for calculating the pathloss. The UEs in the system simulation are static and do not move. A time varying channel is however taken into account by the link-to-system model.

5.2.1.5 Modulation and coding scheme

Since there are different MCSs supported in C-V2X, the network needs to configure the appropriate MCSs for each transmission. An appropriate MCS should meet the data volume requirement

$$\text{SE} \geq \frac{C}{BW} \qquad (5\text{-}2)$$

where SE, C, and BW represent the spectral efficiency of an MCS, the data volume as defined in Section 5.2.1.2, and the allocated bandwidth, respectively. Additionally, since an MCS with a higher spectral efficiency is less robust, the MCS which has the lowest spectral efficiency while fulfilling the condition shown in Eq. (5-2) should be applied. For IVD <= 5, however, even MCS 20 with the highest spectral efficiency does not provide compliance with condition (5-2), and consequently the system is overloaded. This will be addressed further below.

Table 5-1 shows the relations of UE deployment density, data volume and selected MCS index for the case of no retransmission.

Table 5-1: UE deployment, data volume and MCS Parameters for scenarios without retransmission

IVD (m)	#UEs on highway	#UEs on BS coverage	Data volume [Mbps]	MCS index (L2S-1, L2S-2)
3	6928	3464	70.9427	20
5	4156	2078	42.5574	20
10	2078	1039	21.2787	14
20	1039	519	10.6291	7
40	519	259	5.3043	4
50	415	207	4.2394	3
80	259	129	2.6419	1
100	207	103	2.1094	0

For the case of retransmissions, the data volume is effectively doubled and accordingly the required spectral efficiency of the MCS is doubled. This is shown in Table 5-2. For IVD <= 10 m even the MCS 20 with the highest spectral efficiency does not provide compliance with condition (5-2), and consequently the system is overloaded.

Table 5-2: UE deployment, data volume and MCS Parameters for retransmission

IVD (m)	#UEs on highway	#UEs on BS coverage	Data volumes [Mbps]	MCS index (Scenario L2S-3)
3	6928	3464	141.8854	20
5	4156	2078	85.1148	20
10	2078	1039	42.5574	20
20	1039	519	21.2582	14
40	519	259	10.6086	7
50	415	207	8.4788	6
80	259	129	5.2838	4
100	207	103	4.2188	3

In overload scenarios, the eNB is unable to support all the UE's and hence drops some of them. The PRR calculation in this case also considers the dropped UE's. Let PRR_{max} denote the maximal PRR achievable for an overloaded scenario, which is given as the ratio of total number of supported UE's to the total number of UE's within the coverage area of eNB:

$$PRR_{max} = \frac{UE_{supported}}{UE_{eNB}}$$

During simulation runtime, the PRR is calculated only considering the $UE_{supported}$. Let us denote it as $PRR_{runtime}$. $PRR_{runtime}$ is defined as a percentage of UEs that successfully receive a packet from the tagged Tx among the Rxs within the transmission range of the Tx in the running time as shown in Eq. 5-1. The final effective PRR that is shown in the subsequent figures in this chapter is then calculated by multiplying the runtime PRR with the maximum PRR as follows

$$PRR = PRR_{max} * PRR_{runtime}$$

Table 5-3 shows the values of PRR_{max} for different IVD values with and without the use of retransmissions. It can be seen that overloading only happens for IVD < 10 m for the case of no retransmission and IVD < 20 m for the case with retransmission.

Table 5-3: PRRmax for different IVDs with and without Retransmission

IVD	One transmission PRR_{max}	Retransmission PRR_{max}
3	0.2059	0.1029
5	0.3429	0.1714
10	1	0.3419
20	1	1
40	1	1
50	1	1
80	1	1
100	1	1

5.2.2 Results

In this section, the simulation results are presented for the different scenarios and L2S mapping tables. The results are shown in terms of PRR versus IVD graphs. We first start with the simple scenario where all the UEs are constrained to be in one cell area and show the PRR versus IVD for all the L2S mapping tables. We then extend the analysis to the more realistic scenario where the effect of intra-cell interference is considered.

5.2.2.1 L2S-1 (AWGN) for all MCS

In this section we use the link level simulation results from Figure 4-8 that covers the full set of 3GPP defined MCSs, without retransmissions. Since the considered channel is only an AWGN channel, the UE speed does not have any effect on the calculated PRR.

In Figure 5-4, the PRRs of the different transmission frequencies for the sidelink C-V2X communication are plotted. It is easy to find that the PRR of sidelink C-V2X communication increases with raising IVDs from 10 meters to 100 meters, due to the accompanying decrease in MCS index. The PRR value increases from 84.95% to 94.99% when the IVD is increased from 10 meters to 100 meters with 10 Hz transmission rate.

The PRR for different message rates appear to converge about 0.95 with increasing IVD. We provide some contemplation on the expected impact of IVD on the PRR:

1) Wanted received signal power

The wanted received signal power on average is not affected, because it is always evaluating over the same communication range of 400m. However, within the same lane, as the inter-vehicle distance is constant, the distance to the furthest Rx within the communication range does depend on the IVD, but not in a monotonous way. Since each lane has a random offset from the leftmost UE to the left edge of the simulation, the cross-lane wanted received power is further randomized and therefore a noticeable effect of the IVD is not expected.

2) Interference:

Within the same lane, the minimum distance between an Rx and interfering Tx is equal to the IVD, so with increasing IVD the PRR of the worst Rxs should increase. For cross-lane, again due to random offset, the minimum distance can be as small as the lane separation for any IVD, it is just so that for smaller IVD the smaller distances become more probable, but each Tx UE on a small distance has a lower activity ratio, because there is always one active Tx per cell, so the smaller the IVD the more UEs you have the less often one UE is active. So for larger IVD, having an interfering Tx UE at small distance is less probable, but if there is one then it is interfering more often.

3) MCS

The MCS decreases with increasing IVD, because it is determined only according to traffic load. This has the largest effect on the PRR. From Table 5-1 without ReTx the MCS=0 is reached for IVD=100, for 10Hz, so that means the MCS cannot further reduce with further increasing IVD, therefore the PRR is expected to saturate, as the SINR discussion above also does not reveal a clear improvement trend. For lower message rates that MCS 0 is simply reached already for lower IVDs.
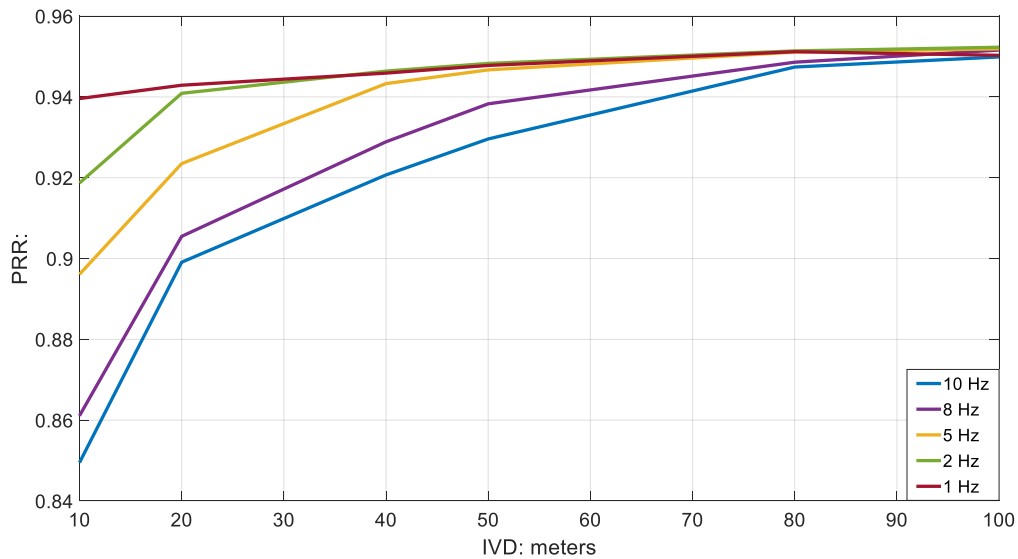
Figure 5-4: PRR vs. IVD for 10 Hz message rate without retransmission for EVA channel

5.2.2.2 L2S-2 and L2S-3 for all MCS with and without Retransmissions

In this section, the system simulation has been carried out for EVA channel for various speeds as outlined in the Appendix A.1 (Figure A-1 to Figure A-6 corresponding to vehicle speeds of 100, 260, 350, 400, 450 and 500 km/h, respectively). The UE deployment, data volume and MCS parameters are similar to the AWGN channel and are outlined in Table 5-1.

Next, the simulation is repeated considering one blind retransmission. The mapping tables are graphically represented in Appendix A.1 (Figure A-7 to Figure A-12). Due to sending the same message twice, the data volume is doubled for the same number of UE's. Effectively, higher order MCS are required to support this higher data volume. The changes of data volume and MCS parameters are outlined in Table 5-2.
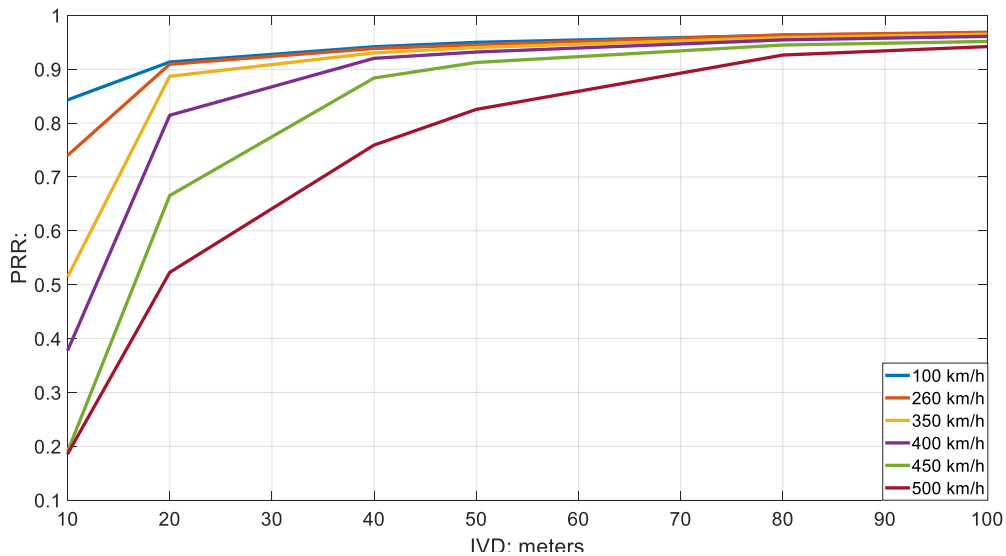
Figure 5-5: PRR vs. IVD for 10 Hz message rate without retransmission for EVA channel

Figure 5-5 and Figure 5-6 show the PRR performance for different speeds for a message frequency of 10 Hz. The following points can be noted

1. For IVD < 10 m, the retransmissions case results in an overloaded scenario as seen by the low PRR. This is also visible in Table 5-2 where the highest MCS is selected for IVD = 10 m. Due to this, the maximum PRR is limited to the total number of supported UE's divided by the total number of UE's present in the network.

2. At high speeds (and consequently high Doppler frequencies), retransmissions have a larger benefit compared to lower speeds. This can be seen in the form of a steeper PRR curve where the retransmission gain is 10 - 15% over the case with no retransmissions for every IVD until 70 m. Above 70 m, due to the lower MCS used, the performance converges.

3. Some aspects of the link and system simulation scenario are expected to lead to lower gains from retransmissions than expected. The first is that always full bandwidth 10 MHz transmissions are assumed, which implies a high degree of frequency diversity to that the time diversity introduced by retransmissions is less relevant. The second is that the system simulation assumes a fully loaded system where there is interference present always in the retransmission, whereas for a different resource allocation scheme this would not be the case.

The simulations have also been carried out for different message frequencies. These results can be found in the Appendix.
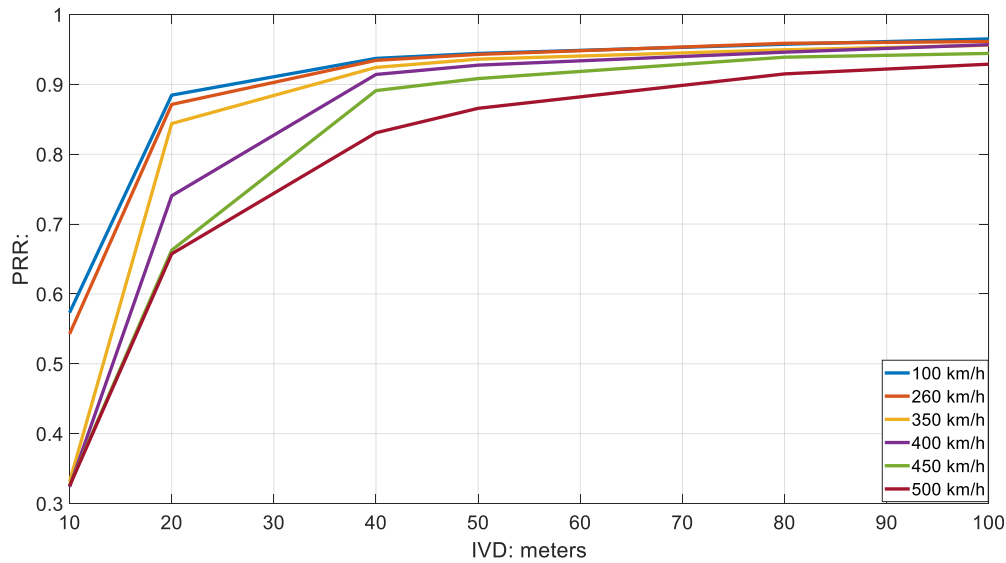
Figure 5-6: PRR vs. IVD for 10 Hz message rate with retransmission for EVA channel

5.2.2.3 Realistic UE deployment model

In the following we drop the constraint that Rx UEs are only evaluated when all of them that are in the communication range of a Tx UE are in the same geometric cell area, and now each Tx UE is controlled by the eNB with the lowest pathloss. The EVA channel mapping tables are applied in this simulation. Moreover, the simulation area is also extended to 7 km with 3 eNBs to have a more realistic interference situation.

Figure 5-7, Figure 5-8, Figure 5-9 show the PRR graphs for the realistic scenario for a message frequency of 10 Hz for different speeds. In addition, the results for 3464-meter and the constraint UE deployment are also added from previous figures for a side by side comparison. We focus the discussion to the scenario for 100 km/h.

It is clear to see that PRR for realistic UE deployment is less that for constrained deployment. Taking both simulations with 3464-meter highway distance as an example, when the IVD is 100 meters, the PRR value decreases from 96.75% to 95.91%.

When we apply an IVD of 100 meters, the PRR for the scenario with 6928-meter highway and 4 eNBs is only slightly less than for the smaller scenario.

When the length of the whole simulation highway is extended to 6928 meters, which means more eNBs are deployed in the communication system, then more Tx UEs are transmitting by using the same resources, so UEs will experience more interference. When we take an IVD of 20 meters, the PRR decreased from 91.34% of simulation with no extension to 89.99% of simulation with extended simulation with 3464-meter highway and further to 89.00% of the simulation with the 6928-meter highway.
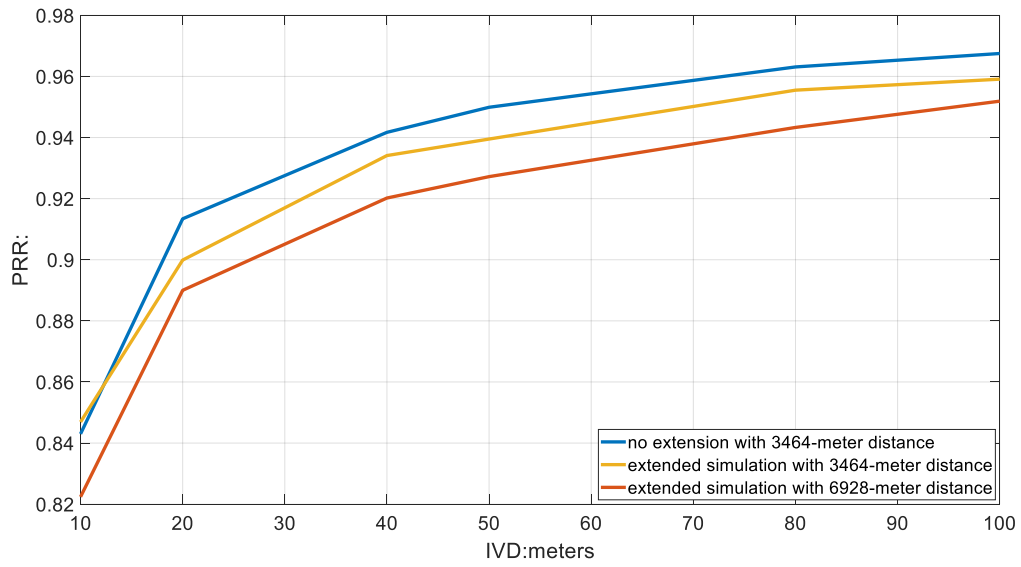
Figure 5-7: PRR comparison for 3464 m and 6928 m highway scenarios with 100 km/h EVA channel mapping table
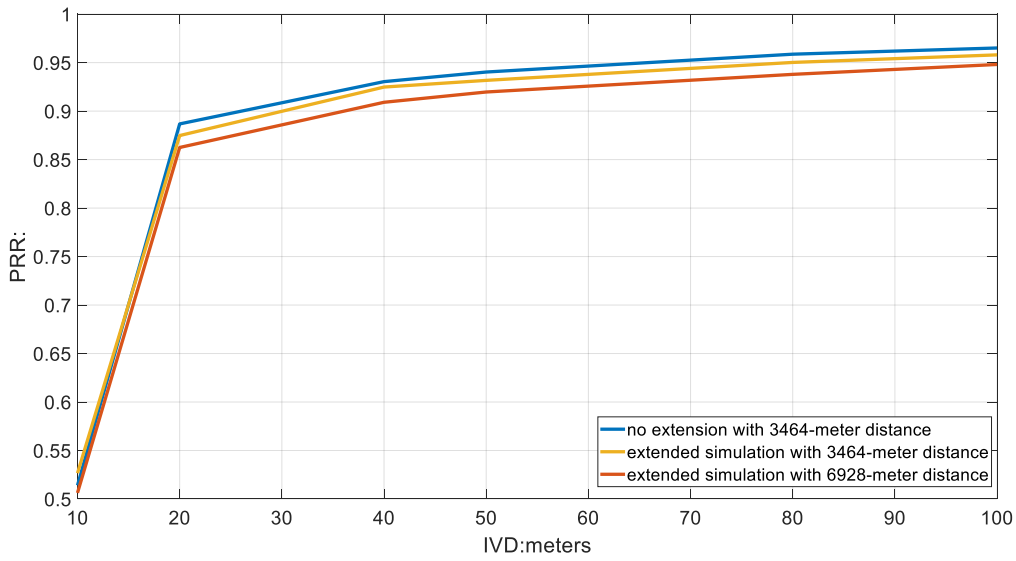
Figure 5-8: PRR comparison for 3464 m and 6928 m highway scenarios with 350 km/h EVA channel mapping table
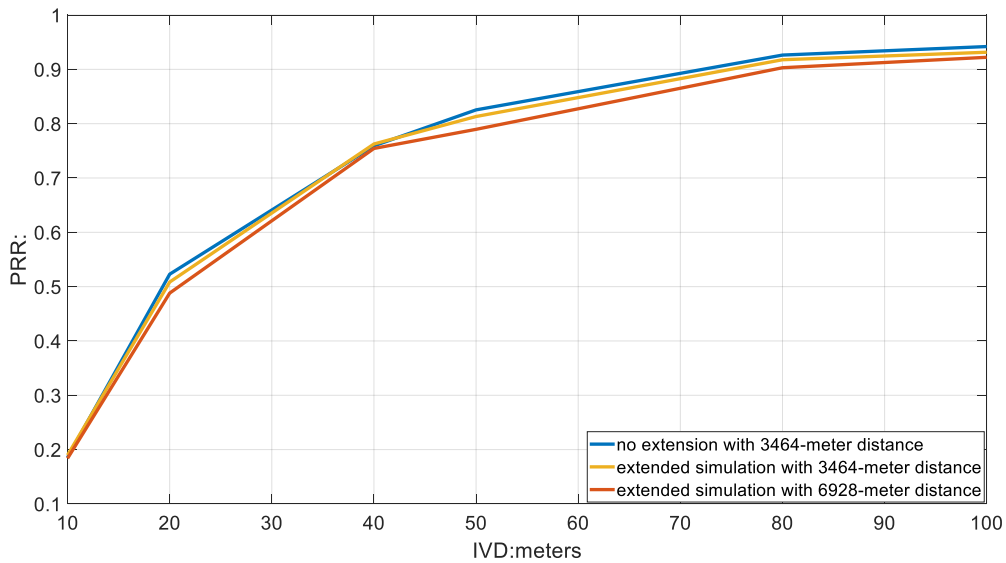

Figure 5-9: PRR comparison for 3464 m and 6928 m highway scenarios with 500 km/h EVA channel mapping table

5.3 Real World System: Mode 4 instead of Mode 3

As mentioned in 5.1. there are the two different PC5 sidelink transmission modes defined, and while the simulation work here was done assuming mode 3, in reality mode 4 is used in the field and supported by automakers and semiconductor suppliers throughout the world.

The conclusions seen from the system level analysis on LTE-V2X sidelink "mode-3" is that it suffers from performance issues in addition to a number of added complex requirements and business considerations. As such, the preferred technology for direct communications is LTE-V2X sidelink "mode-4" which does not require the network for the sake of resource control.

Mode3 would mean that the resources for the direct communication on the PC5 link are scheduled by a eNB, which has further implications: the actual control information for this task would be transferred to the normal LTE cellular system and spectrum, which means the mobile network operators would need to get involved and likely charge for this service. Furthermore, agreements would need to be reached which operator is taking the responsibility, since all UEs in the vehicles need to be controlled by the same network, yet different vehicle manufacturers have relationships with different mobile network operators. The introduction of mode 3 support to the eNBs means additional cost, complexity and requires eNB software upgrades. Furthermore, ubiquitous coverage would be required. Apart from sidelink resource control the network does have a valued role in connected vehicles.

The simulations showed that there are quite some challenges or inferior results regarding the capacity if an easy implementation is assumed. The eNB schedulers would need much more knowledge about the individual UEs and how they experience their environment to be able to re-use the resources for UEs that do not interfere with each other, and avoid collisions between UEs close to each other. Since for Mode 4 the resource selection is autonomous for each UE or distributed from a system point of view, this knowledge about the environment for such decisions is already there by the design: each UE is permanently monitoring and ranking the resources, and does resource selections and reselections based on this, taking the lowest loaded locations in the frequency and time domain. Furthermore congestion control algorithms are kicking in in highly loaded situations that guarantee a still working system in particular for the intended safety applications. Getting detailed UE based information to the scheduler would create additional overhead in the uplink plus complexity on the UE and of course the eNBs.

A further challenge for Mode 3 that was mentioned but not simulated would be, that handovers between the eNBs in control would be needed, likely connected with interruption times, which translate into no communication for some time. This might not be acceptable for safety applications.

There is the possibility to move over to Mode 4 in such cases, and similar when there is no coverage from the eNBs, however in a mixed operation the resource selection of the Mode 3 part would be suboptimal even when complex feedback might be implemented, because there will be no knowledge about the Mode 4 UEs which can lead to colliding resource assignments.

Due to the simpler design providing good or even better performance, Mode 4 is chosen for the actual implementation. Its support is mandated by the standard for C-V2X devices and preferred by automakers.

6 Summary and Conclusions

In this report, C-V2X sidelink and ITS-G5 technologies have been evaluated for their link level performance. Additionally C-V2X sidelink in the network controlled mode ("mode 3") was evaluated for system performance and subsequently conclusions drawn comparing it to "mode 4" where PC5 sidelink autonomously selects a radio resource.

Link level performance of C-V2X is typically 4 - 6 dB better than for ITS-G5 for low speeds and in the case without retransmission, of which only C-V2X is capable. The link performance of C-V2X is further significantly improved by retransmissions, in particular for higher speeds of 350 to 500 km/h. For instance, at a target BLER of 10% the gain due to retransmission is 6 dB at 400 km/h. For 500 km/h a target BLER of 10% cannot be reached without retransmission unless for the 3 most robust MCSs. For speeds of 100 to 260 km/h the additional gain of retransmission is about 3.5 dB for MCSs using QPSK.

On the system level, this report has investigated C-V2X "mode 3", where the resource allocation for the direct V2V communication is performed by eNBs. For a message rate of 10 per second, the Packet Reception Ratio PRR is above the 90% target for all Inter-Vehicle-Distances IVD above 40m and UE speeds up to 400 km/h when the MCS is optimally chosen. For 500 km/h this is only the case for IVD above 80 m, however, given the high speed the breaking distance does also require such high IVD.

With a single retransmission, the load is naturally doubled and accordingly less robust MCS is used. There are hardly any simulation scenarios where retransmissions can lift the PRR above the target of 90%. However, some aspects of the link and system simulation scenario are expected to contribute to that the retransmissions do not harvest the full diversity gain potential. At high speeds retransmissions do increase the PRR by 10 - 15%, however, still only at an unacceptably low level.

The baseline system simulation results have been obtained for a system consisting of only 2 eNBs and with some simulation-friendly restrictions on UE deployment. However, for the most relevant scenarios the simulations have been repeated with larger system size and realistic UE deployment and eNB association and the PRR declined by at most 2%-points. The conclusions seen from the system level analysis on LTE-V2X sidelink "mode-3" is that it suffers from performance issues in addition to a number of added complex requirements and business considerations. As such, the preferred technology for direct communications is LTE-V2X sidelink "mode-4" which does not require the network for the sake of resource control.

Appendix

Appendix A Simulation setup

Appendix A.1 Link Level Simulation – Extended Results

In this section, the extensive link level simulation results are documented. We use EVA Channel model as the baseline model and plot the BLER versus SNR (in dB) link level results for different speeds for all C-V2X MCS schemes in Figure A-1 to Figure A-12.
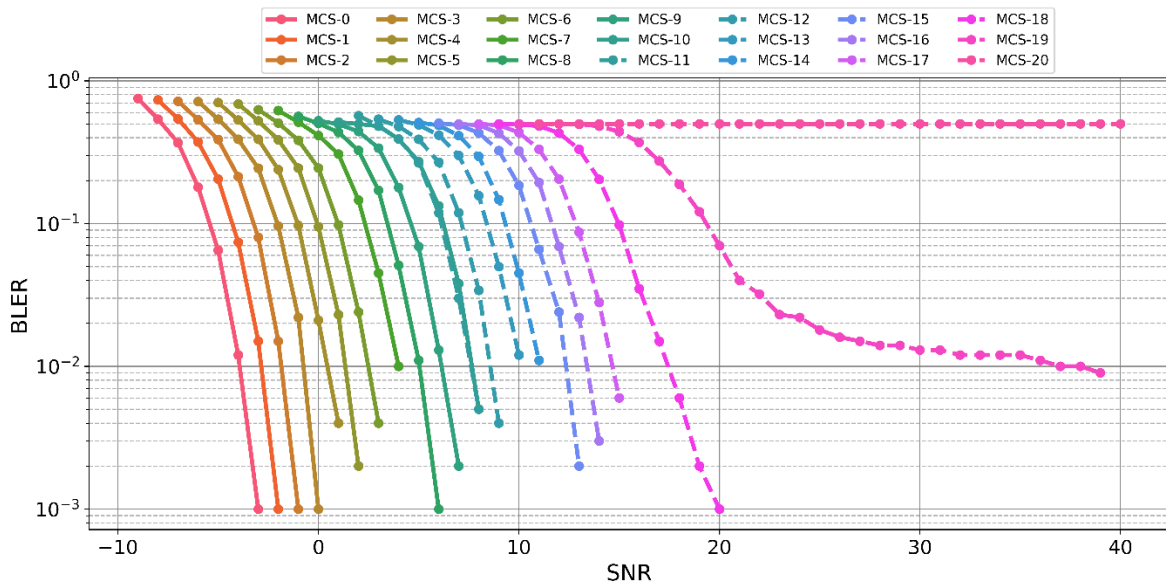
Without Retransmission (1X2 SIMO)

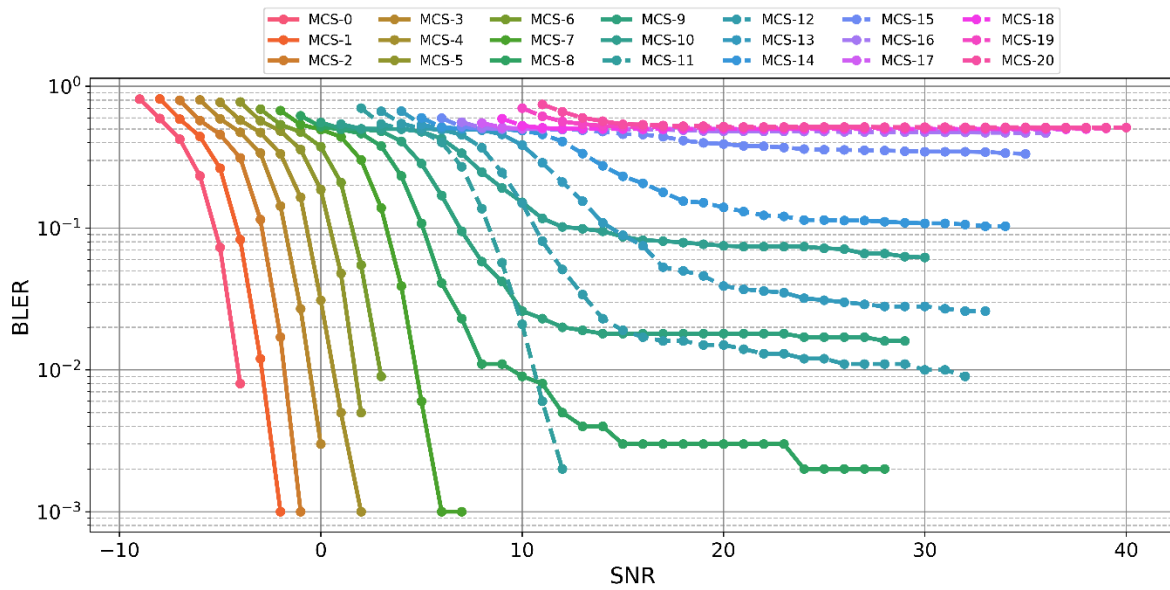*Figure A-1: C-V2X Performance for EVA Channel at 100 km/h (Without retransmission)*

Figure A-2: C-V2X Performance for EVA Channel at 260 km/h ((Without retransmission))
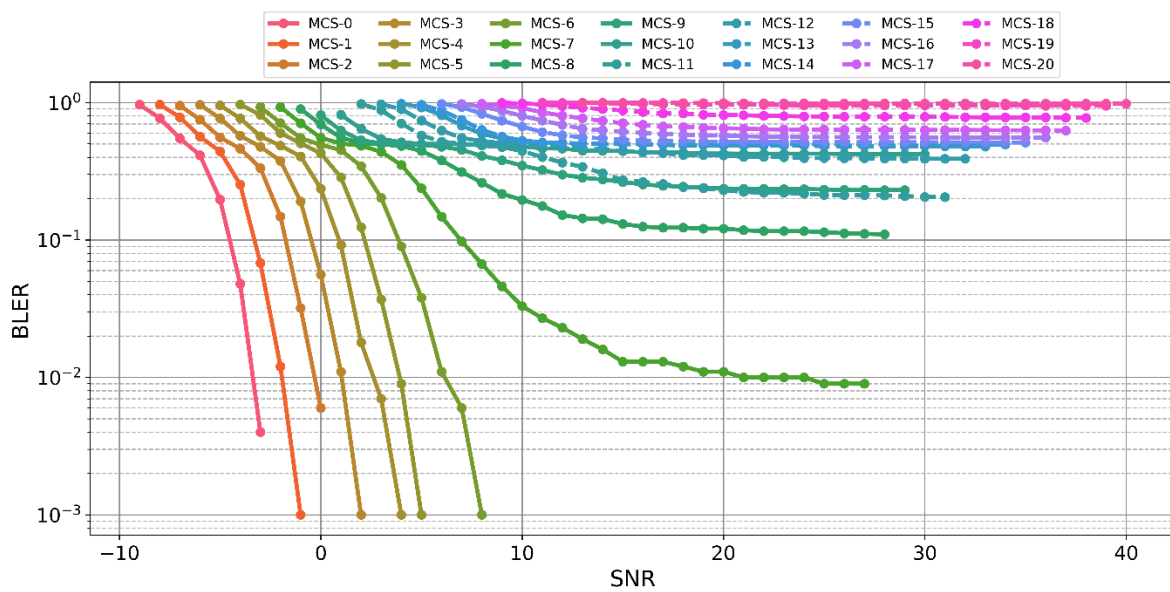
Figure A-3: C-V2X Performance for EVA Channel at 350 km/h (Without retransmission)
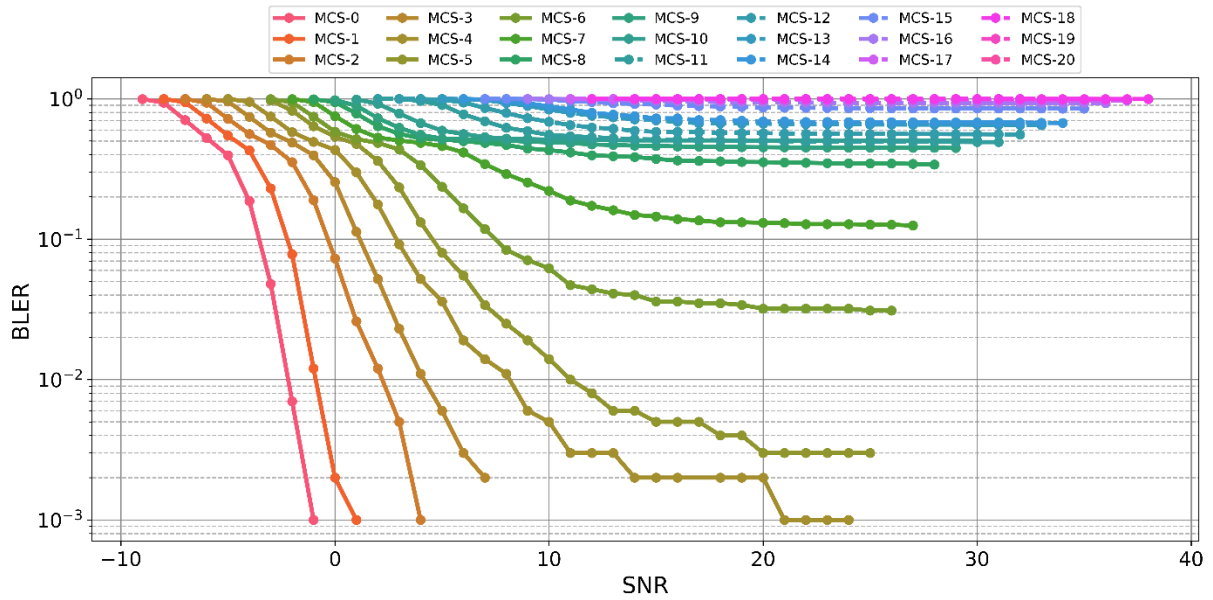
Figure A-4: C-V2X Performance for EVA Channel at 400 km/h (Without retransmission)
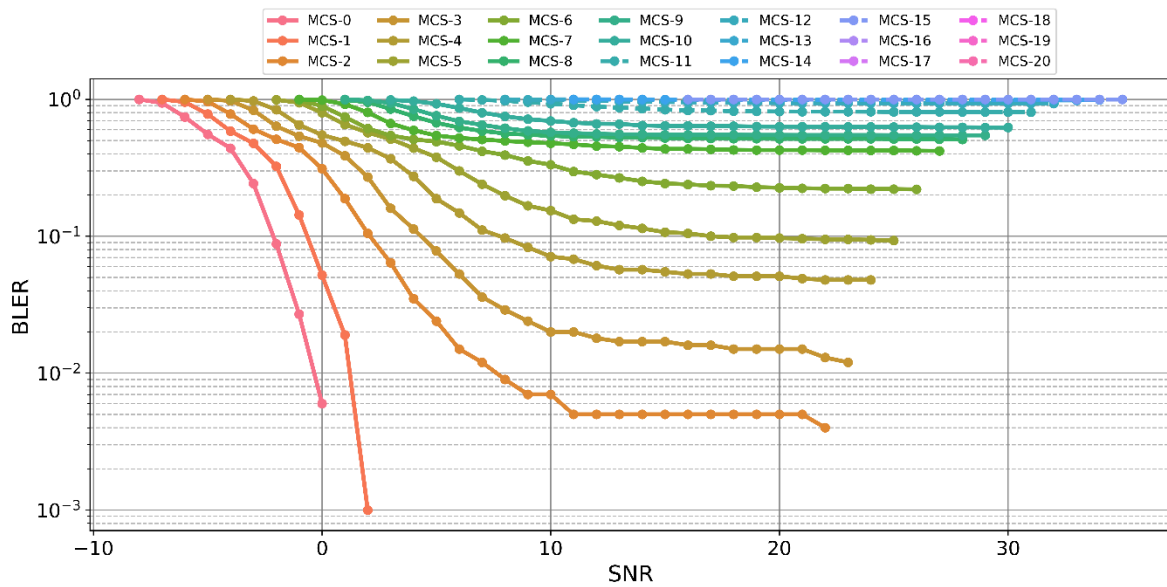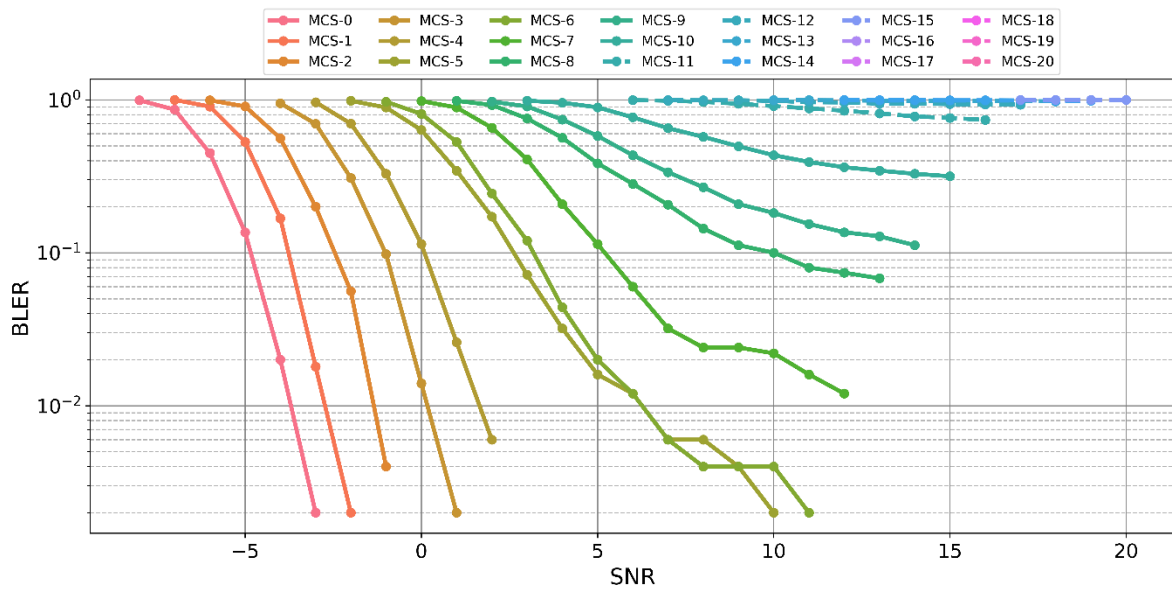

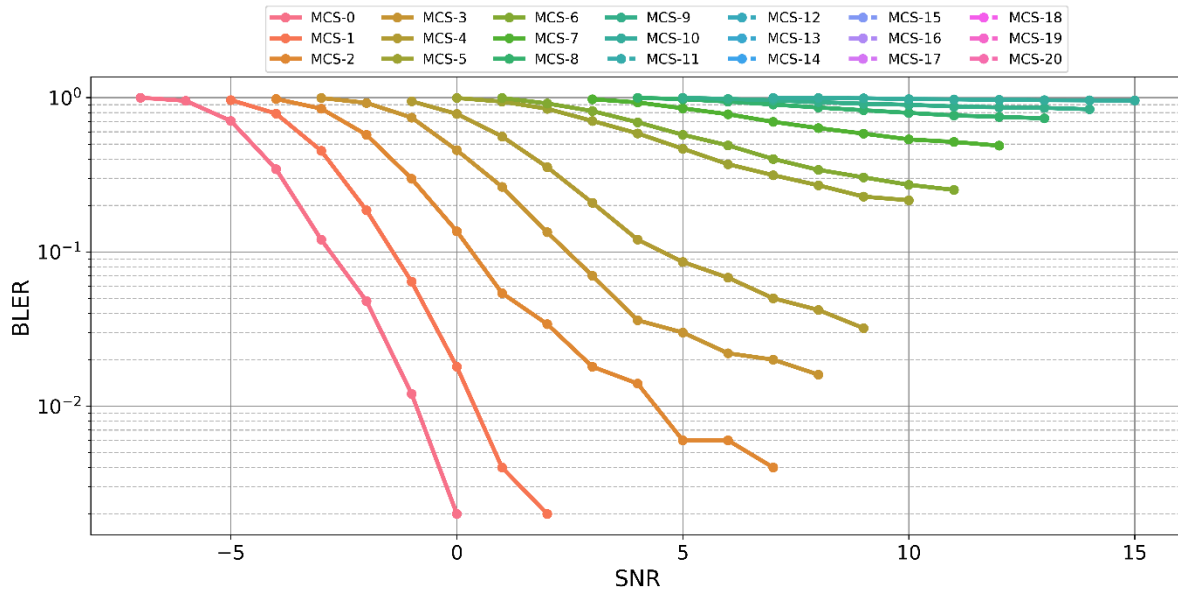*Figure A-5. C-V2X Performance for EVA Channel at 450 km/h (Without retransmission)*
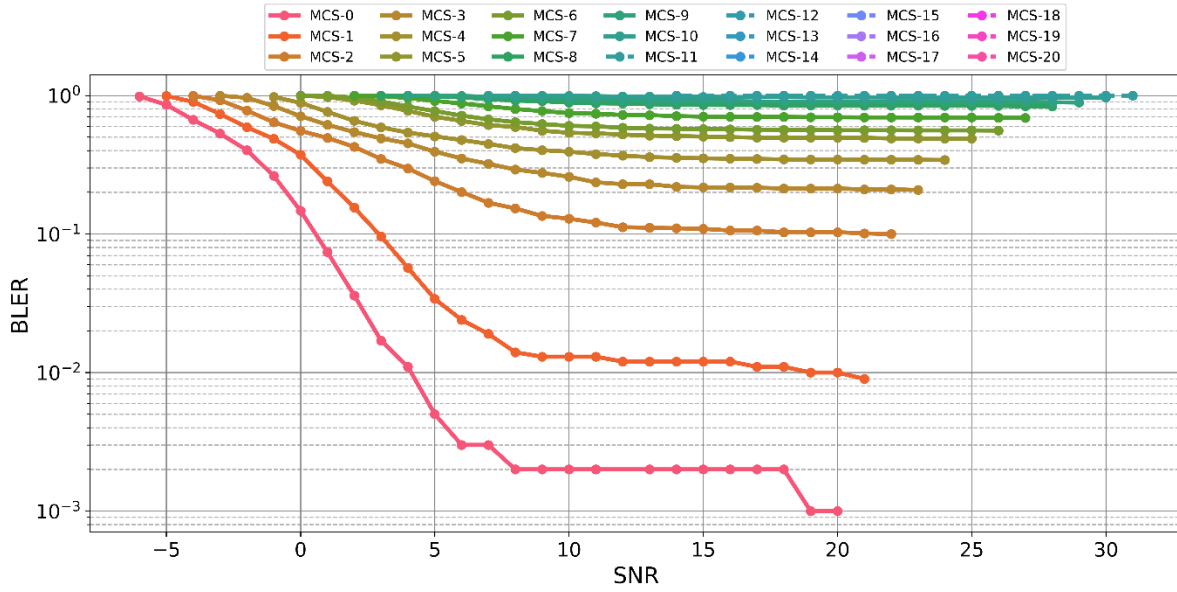
Figure A-6: C-V2X Performance for EVA Channel at 500 km/h (Without retransmission)

With 1 blind retransmission (1X2 SIMO)
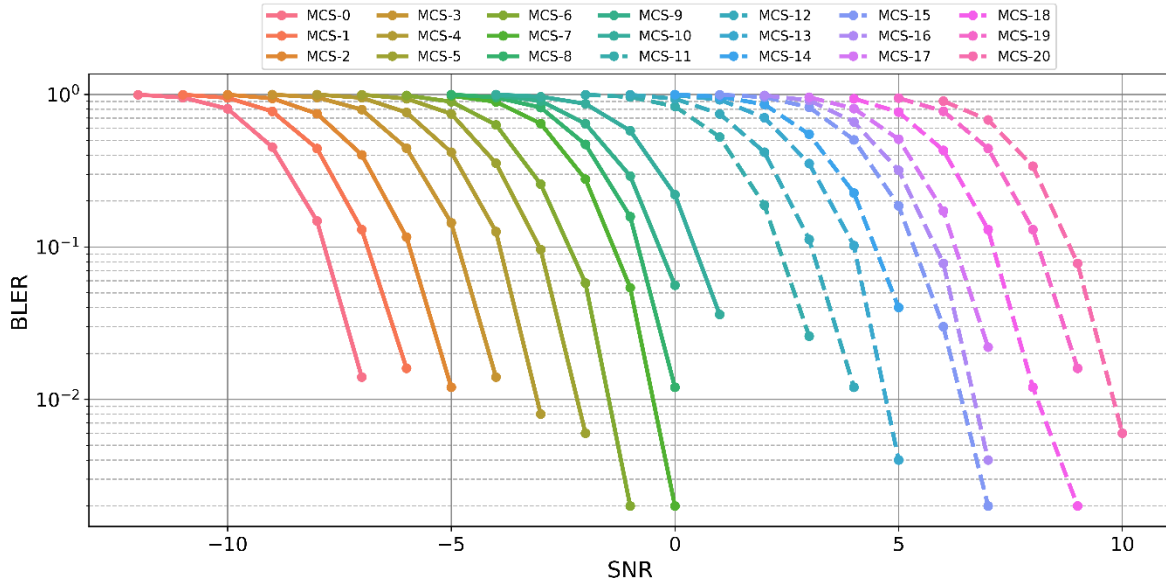
Figure A-7: C-V2X Performance for EVA Channel at 100 km/h (With retransmission)
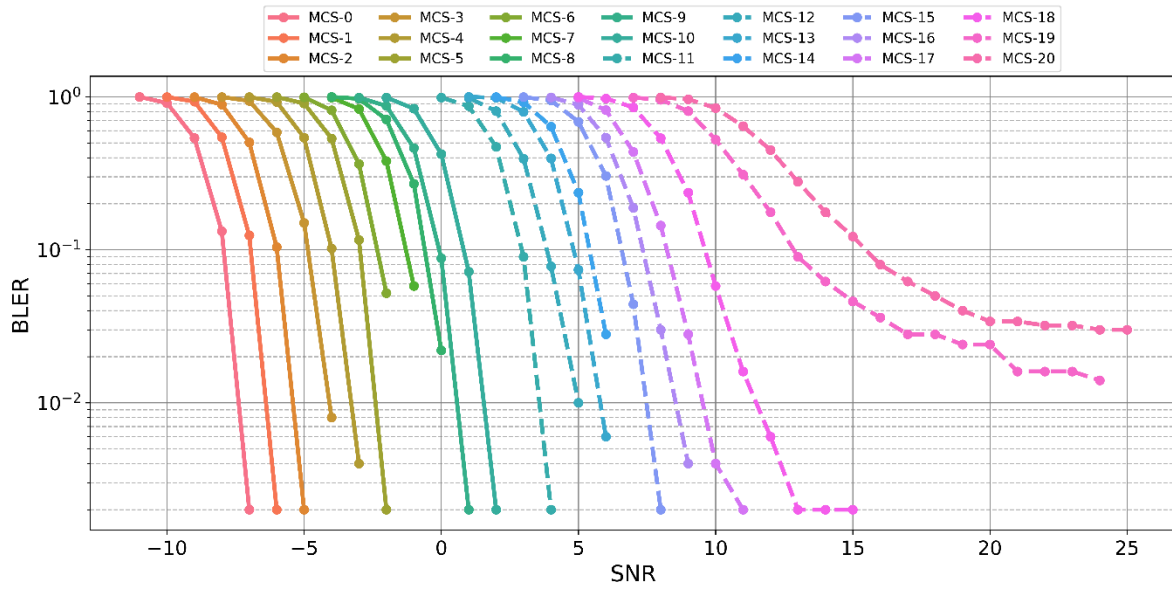
Figure A-8: C-V2X Performance for EVA Channel at 260 km/h (With retransmission)
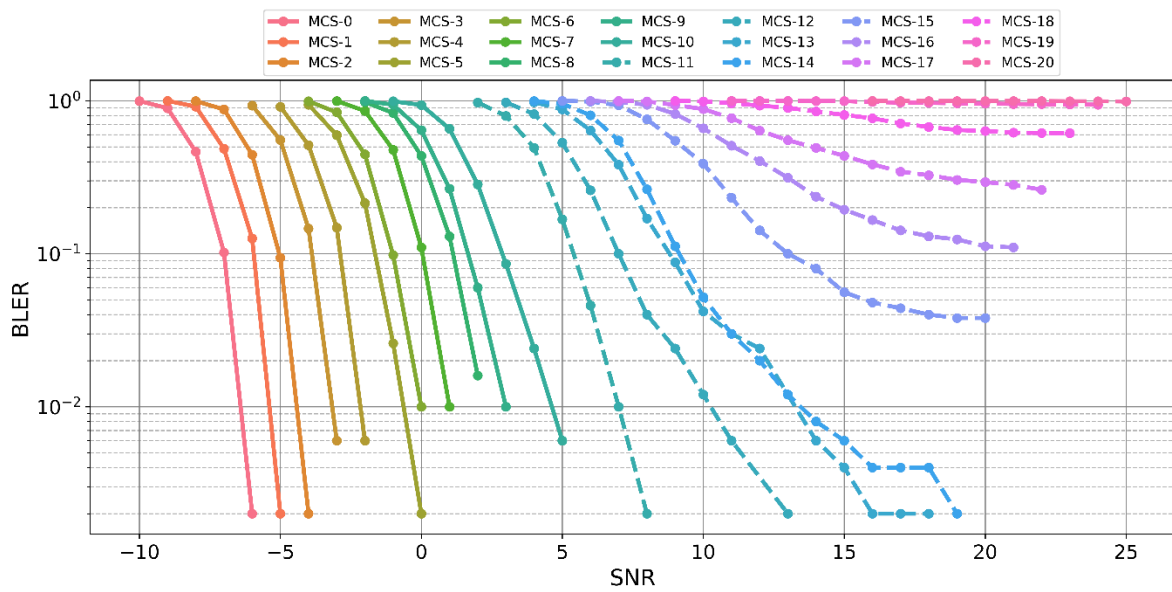
Figure A-9: C-V2X Performance for EVA Channel at 350 km/h (With retransmission)
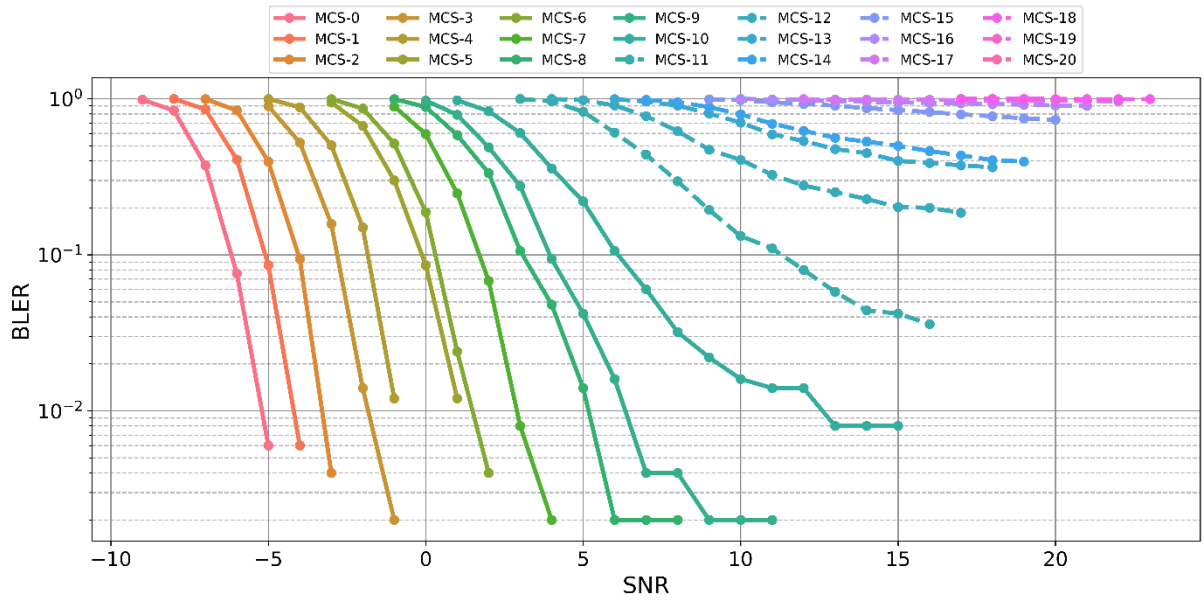
Figure A-10: C-V2X Performance for EVA Channel at 400 km/h (With retransmission)

Figure A-11: C-V2X Performance for EVA Channel at 450 km/h (With retransmission)

Figure A-12: C-V2X Performance for EVA Channel at 500 km/h (With retransmission)

Appendix A.2 System Level Simulation – Extended Results

In this section, system level simulation results in the form of PRR versus IVD are documented for various messages frequencies and vehicle speeds in Figure A-13 to Figure A-24. Note that the curves for 10 Hz message frequency from all these figures are combined together and discussed in Section 5.2.2.2.

EVA Channel for all MCS without Retransmissions for different message frequencies
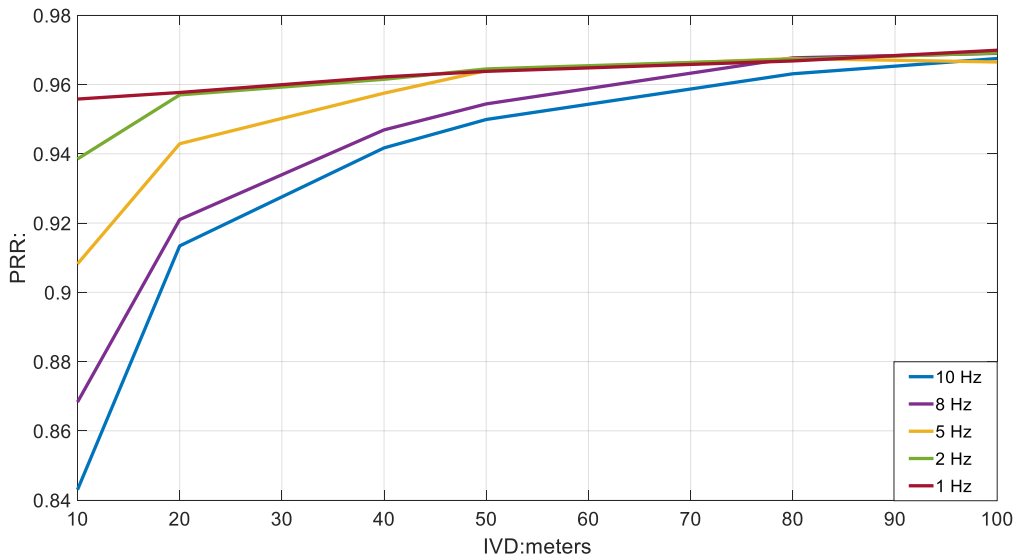
Figure A-13: PER for 100 km/h without retransmission for EVA Channel
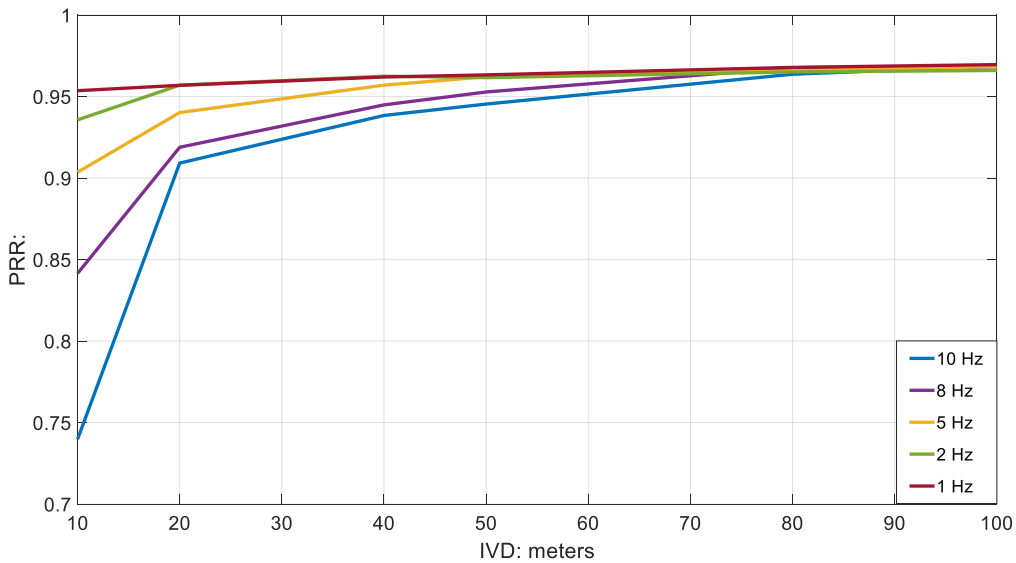
Figure A-14: PER for 260 km/h without retransmission for EVA Channel
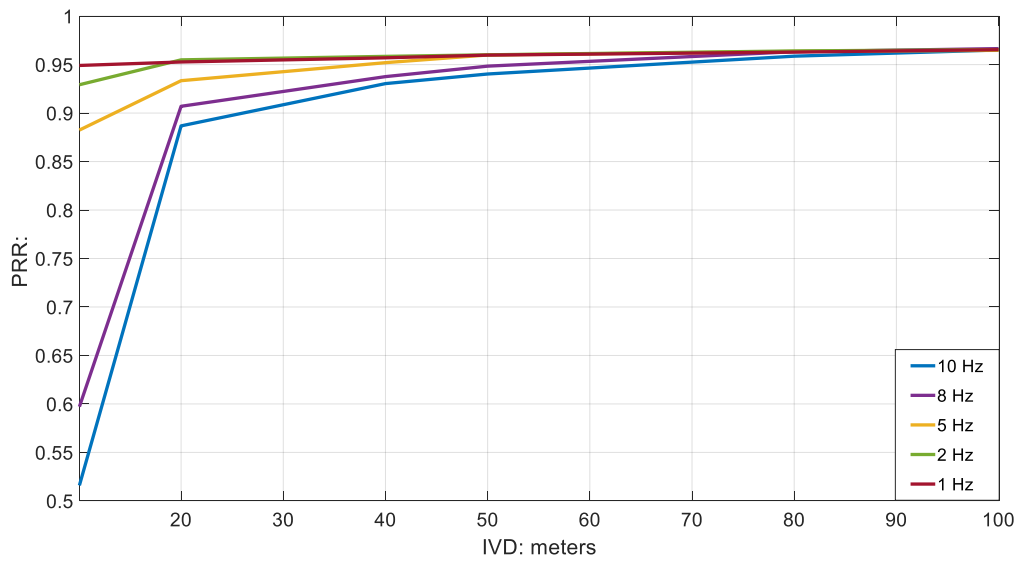
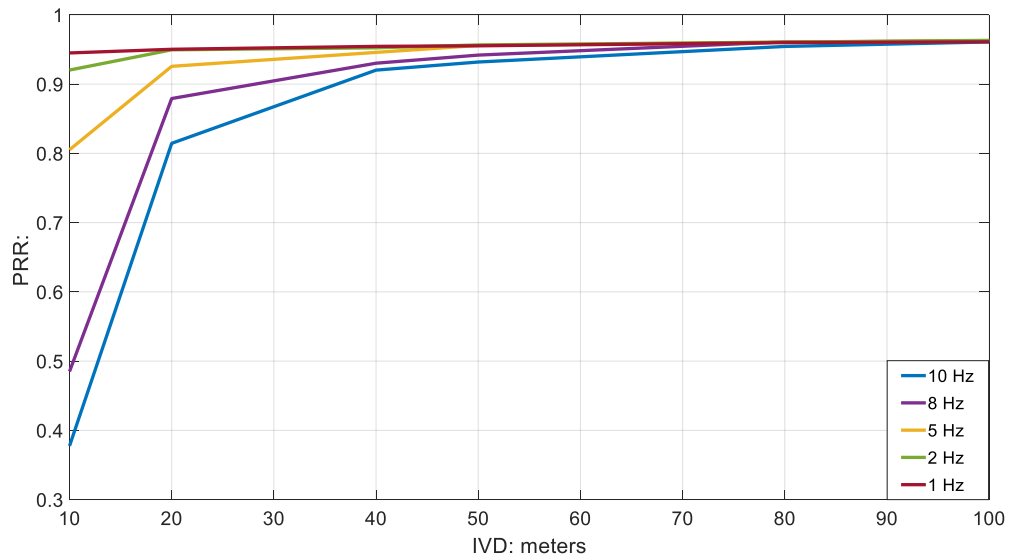*Figure A-15: PER for 350 km/h without retransmission for EVA Channel*

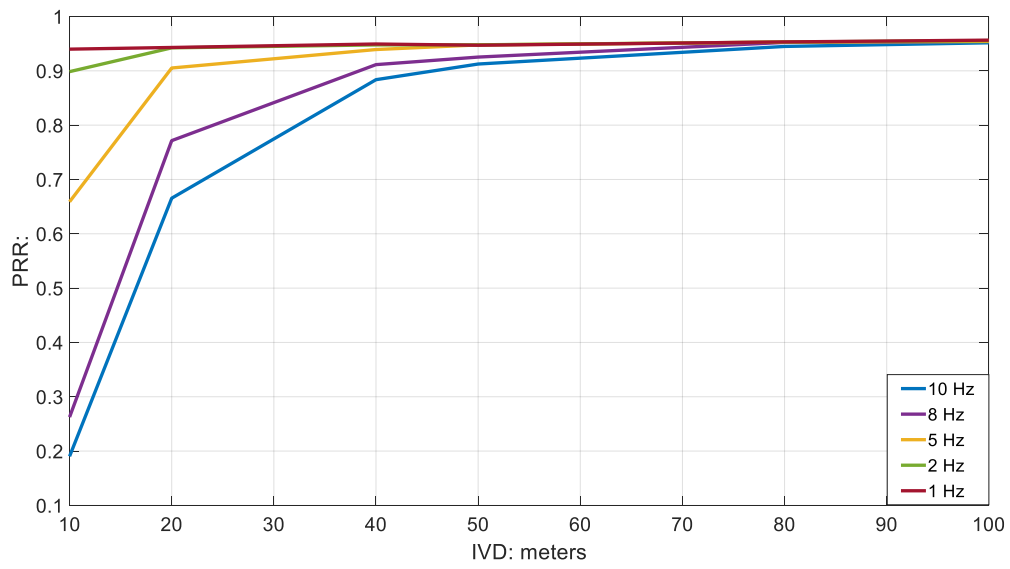*Figure A-16: PER for 400 km/h without retransmission for EVA Channel*

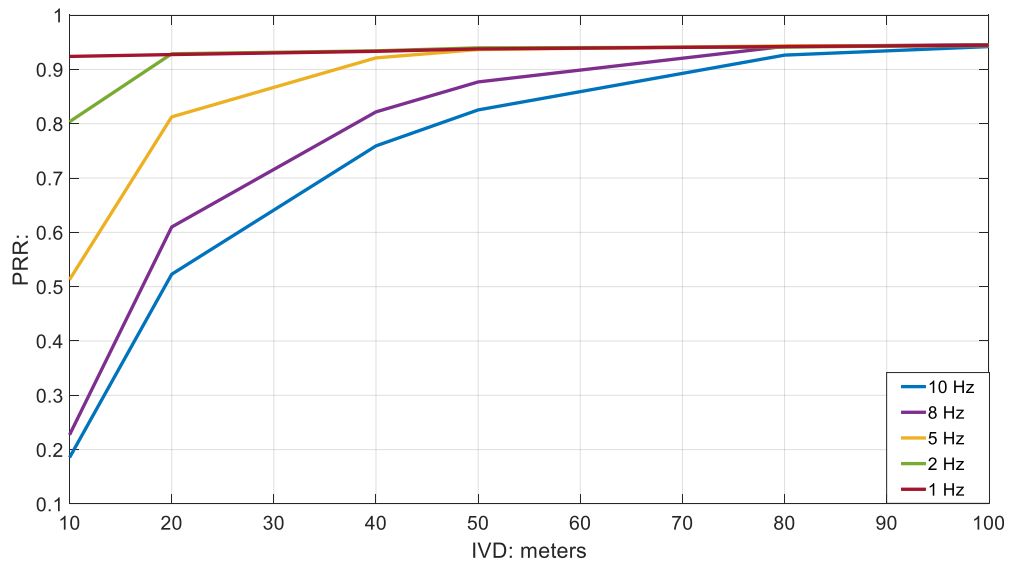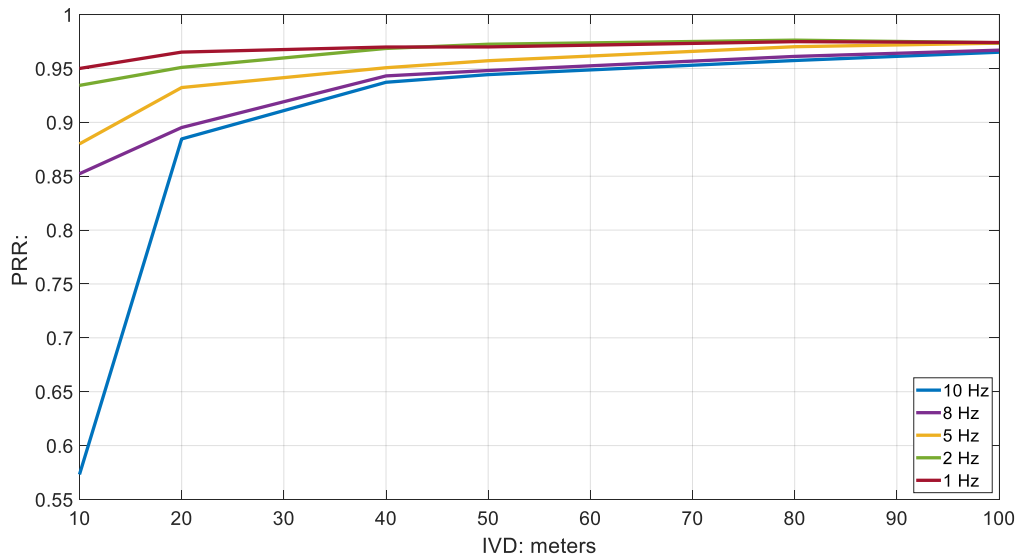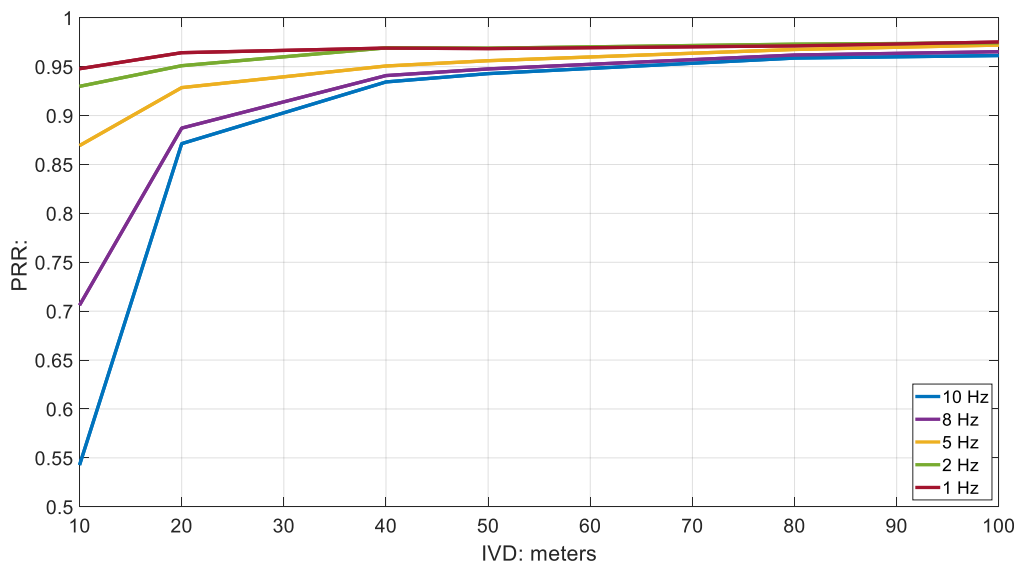*Figure A-17: PER for 450 km/h without retransmission for EVA Channel*

Figure A-18: PER for 500 km/h without retransmission for EVA Channel

EVA Channel for all MCS with retransmissions

Figure A-19: PER for 100 km/h with retransmission for EVA Channel

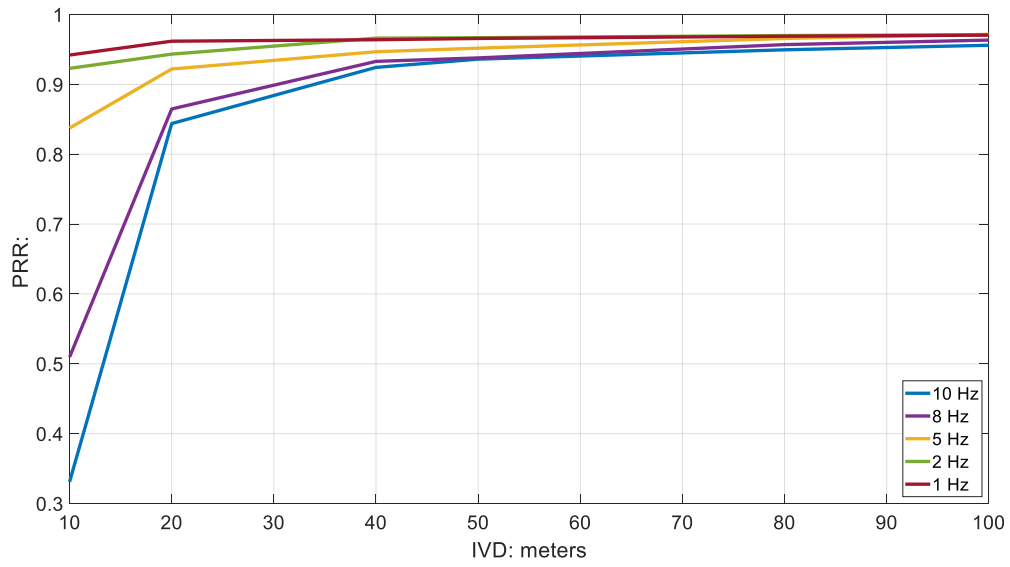*Figure A-20: PER for 260 km/h with retransmission for EVA Channel*

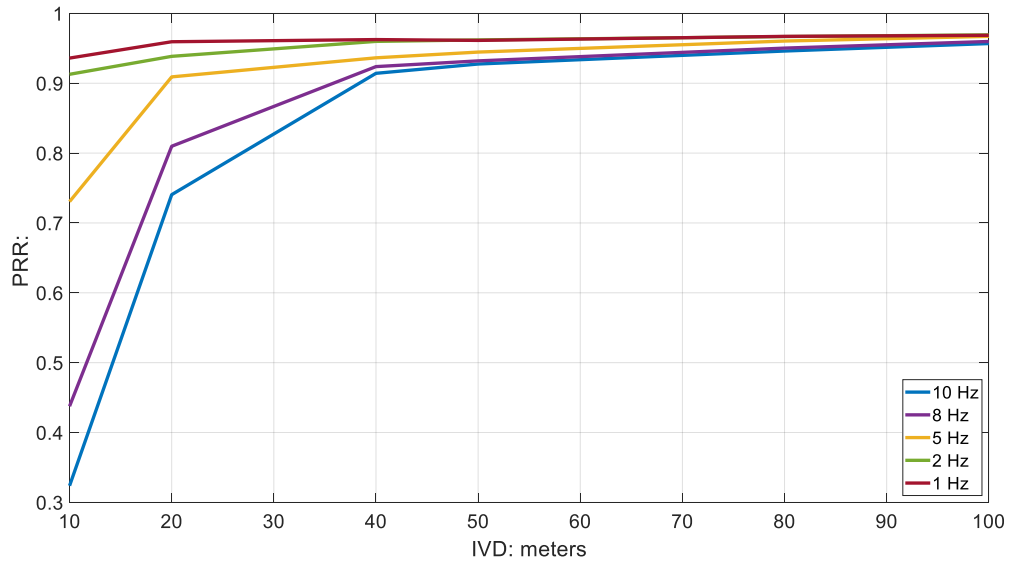*Figure A-21: PER for 350 km/h with retransmission for EVA Channel*

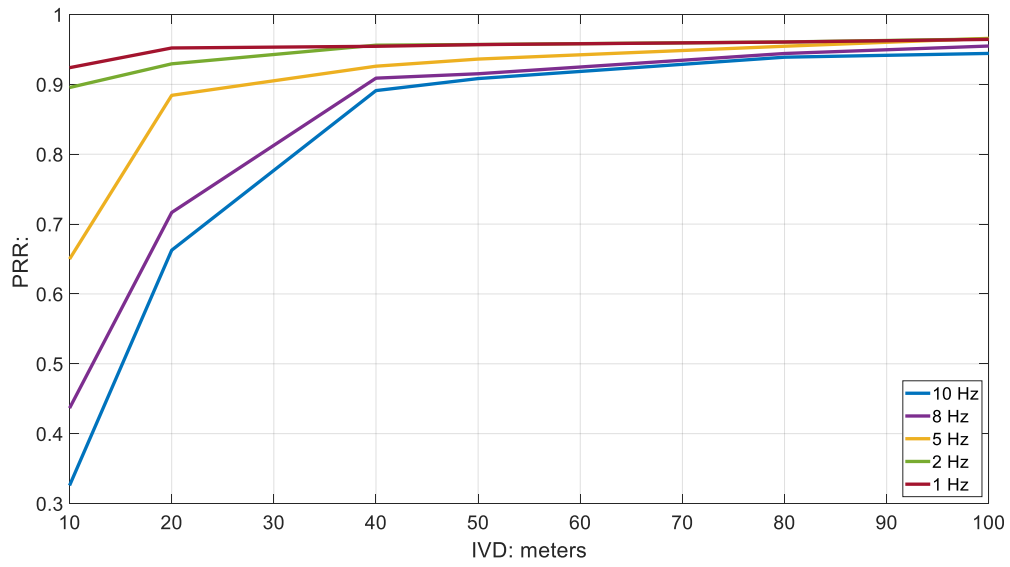*Figure A-22: PER for 400 km/h with retransmission for EVA Channel*

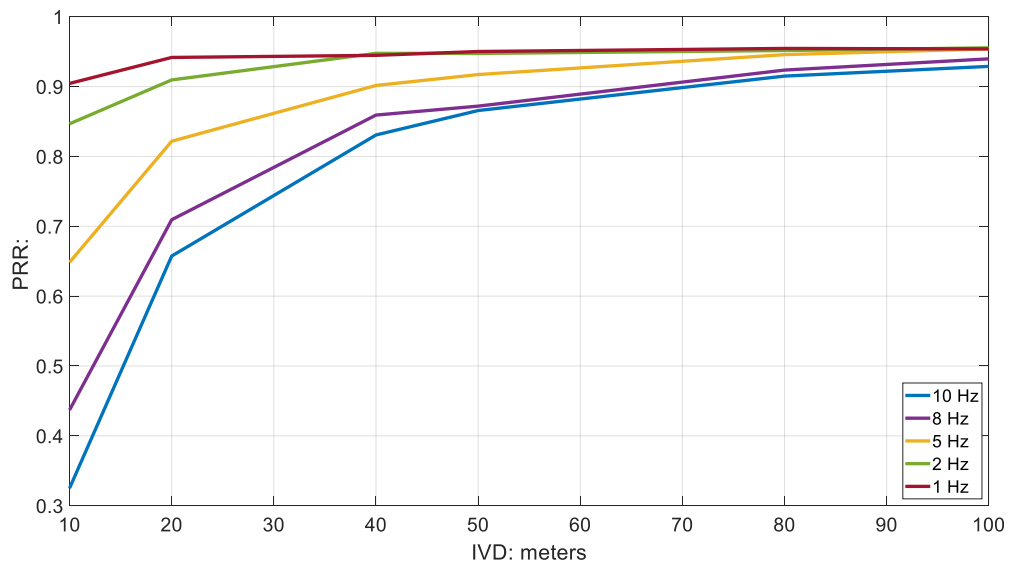*Figure A-23: PER for 450 km/h with retransmission for EVA Channel*

Figure A-24: PER for 500 km/h with retransmission for EVA Channel

Simulation of QPSK 1/3 for different speeds without retransmissions

In this section, we use the reference channel as outlined in Section 4.4.2 which uses QPSK with coding rate 1/3. The corresponding mapping table is shown in Figure 4-22. Due to using a fixed MCS scheme, the number of UE's supported is also limited. The number of PRBs required for one sidelink transmission is calculated as

$$NPRB_{PSSCH} = \frac{ps * 8}{N_{sc\_rb} * s_u * m * c} \approx 29$$

Where N_{rb_sc} is the number of sub-carriers in one resource block (12),), m is the modulation order (bits per symbol for QPSK =2), c is the coding rate (1/3), ps is the packet size in bytes (256), and s_u is the number of usable symbols per one OFDM symbol (9). The total number of PRBs required to transmit one message is the sum of PRBs required for transmission of both PSSCH and PSCCH (2)

$$NPRB_{tot} = NPRB_{PSSCH} + NPRB_{PSCCH} = 31$$

Given a total of 50 PRBs in one subframe, the number of UEs that can be scheduled in one subframe is then given as

$$n\_ue_{sf} = \frac{50}{NPRB_{tot}} \approx 1.61$$

Therefore, the total number of $UE_{supported}$ per second is then calculated as

$$UE_{supported} = \frac{n_{ue_{sf}} * n_{sf}}{ps_f} = \frac{1.61 * 1000}{10} = 161$$

Hence, a total of 161 UEs with a message frequency of 10 can be scheduled within one second.

Table A-1 outlines the UE deployment parameters in terms of the number of supported UE's and the maximum PRR which is calculated as explained in 5.2.2.2. The final PRR is obtained by multiplying the PRR obtained from simulation, $PRR_{runtime}$ with the maximum PRR, PRR_{max}.

Table A-1: UE Deployment parameters for QPSK 1/3 with no retransmission

IVD (m)	#UEs on highway	#UEs on BS coverage	#UEs in Tx range	UE_supported	PRRmax
5	4156	2078	960	161	0.0775
10	2078	1039	480	161	0.1550
20	1039	519	240	161	0.3102
40	519	259	120	161	0.6216
50	415	207	96	161	0.7778
80	259	129	60	161	1
100	207	103	47	161	1

Figure A-25 shows the *PRR* for different vehicle speeds using the QPSK 1/3 mapping table. When an IVD value of 10 meters is applied, the system is obviously overloaded. Since 161 UEs were supported, the *PRR* value is only 11.90% when 500 km/h is used. If the system can support all UEs in the communication range, the *PRR* is higher. For instance, when we apply the IVD of 100 meters, the *PRR* value is 73.7% with 500 km/h speed.
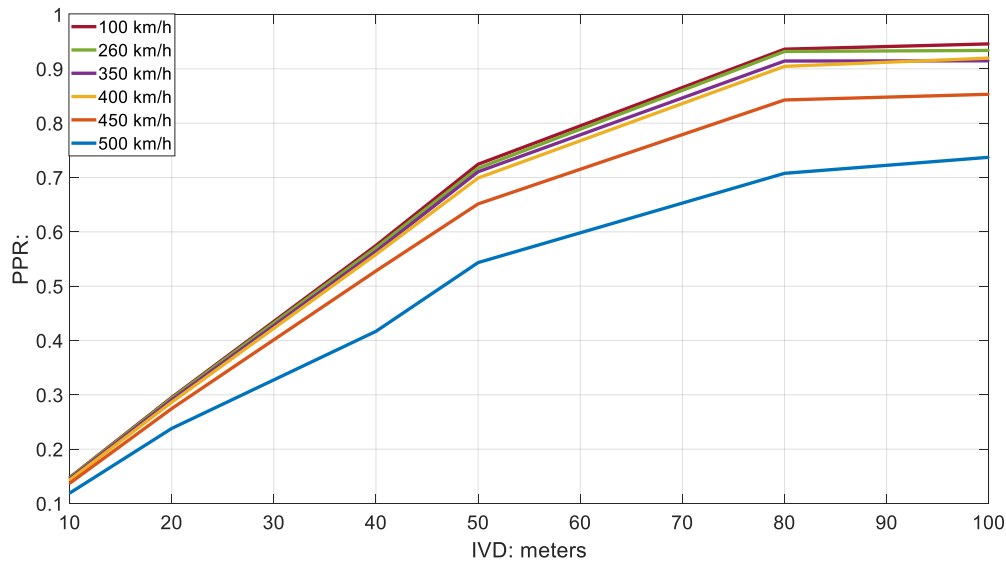
Figure A-25: PRR for QPSK 1/3 without retransmission

It is clear that the *PRR* decreases with increased mobile velocities because of the Doppler effect. For instance, for a sidelink C-V2X communication with an IVD value of 100 meters, the *PRR* is 94.6% for a velocity of 100 km/h. However, if we increase the velocity to 500 km/h, then the *PRR* is 73.7%.

Simulation of QPSK 1/3 for different speeds with retransmissions

We use the same constellation parameters as with the previous section. Because of the use of retransmissions, twice as many messages are transmitted every second by each UE. Therefore, $UE_{supported} = 80$ which is half compared to the simulation without retransmissions. Since less of UEs are supported more UEs are dropped in the case with retransmission.

Table A-2: UE deployment parameters for QPSK 1/3 with retransmission

IVD (m)	#UEs on highway	#UEs on BS coverage	#UEs in Tx range	UE_supported/2	PRRmax
5	4156	2078	960	80	0.0385
10	2078	1039	480	80	0.0770
20	1039	519	240	80	0.1541
40	519	259	120	80	0.3089
50	415	207	96	80	0.3865
80	259	129	60	80	0.6202
100	207	103	47	80	0.7767

In Figure A-26, the retransmission simulation results are plotted. For IVD of 10 meters, because of retransmissions, only 80 UEs are supported. The *PRR* is 7.5% for 500 km/h speed which is less than the result of 11.9% from Figure A-25 for the same IVD and speed. Although retransmission is applied, the benefit of retransmission is compensated by few number of supported UEs.

The *PRR* value has decreased with increased mobile velocities because of the same Doppler effect. Obviously, with a higher velocity, the Doppler effect on communication will also become larger and if the velocity decreases, the Doppler effect on communication will decrease too. For instance, for a sidelink C-V2X communication with an IVD value of 100 meters, we get the *PRR* value of 77.4% when the velocity is 100 km/h. However, if we increase the velocity to 500 km/h, then the *PRR* value is 75.5%.
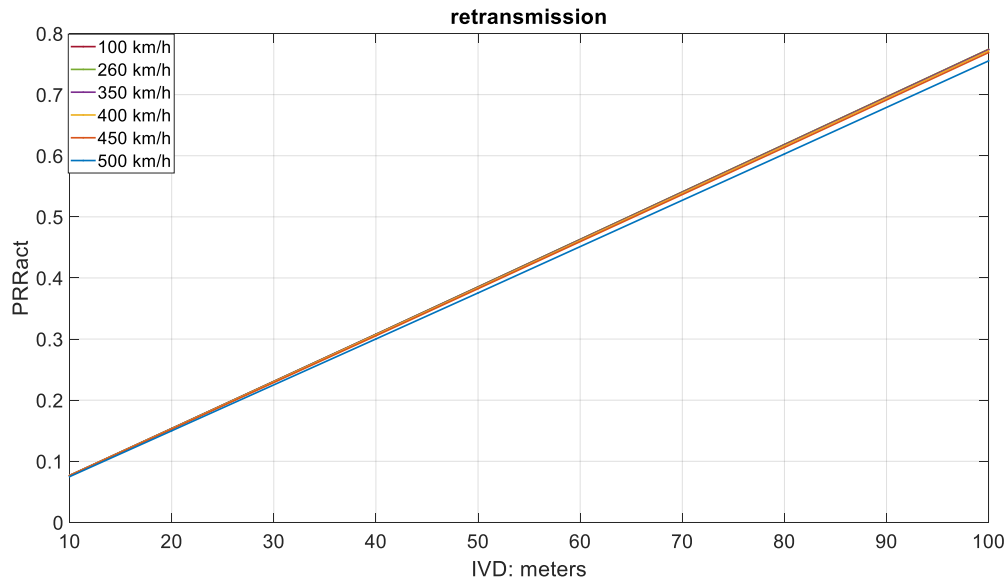

Figure A-26: PRR for QPSK 1/3 with retransmission

In order to compare the simulation performances between one transmission and retransmission, Table A-3 and Table A-4 are provided showing $\text{PRR}_{runtime}$, PRR_{max}, and *PRR* values for an evaluating speed of 100 km/h in. As mentioned before, $\text{PRR}_{runtime}$ is the ratio of the UEs in the communication range of the Tx receiving data packets successfully and the total number of UEs in the communication range of the Tx. Since retransmission is applied, the $\text{PRR}_{runtime}$ value is increased from 95.2% without retransmission to 99.70% with retransmission when an IVD value of 10 meter is applied. It's easy to tell when retransmission is utilizing, the performance of the communication system is increased from $\text{PRR}_{runtime}$ side.

Table A-3: PRR values for 100 km/h without retransmission

IVD/Velocity	#UEs on BS coverage	UE-supported	PRR_{max}	$PRR_{runtime}$	PRR
10	1039	161	0.1550	0.9520	0.1476
20	519	161	0.3102	0.9518	0.2952
40	259	161	0.6216	0.9249	0.5749
50	207	161	0.7778	0.9314	0.7244
80	129	161	1	0.9362	0.9362
100	103	161	1	0.9459	0.9459

Table A-4: PRR values for 100 km/h with retransmission

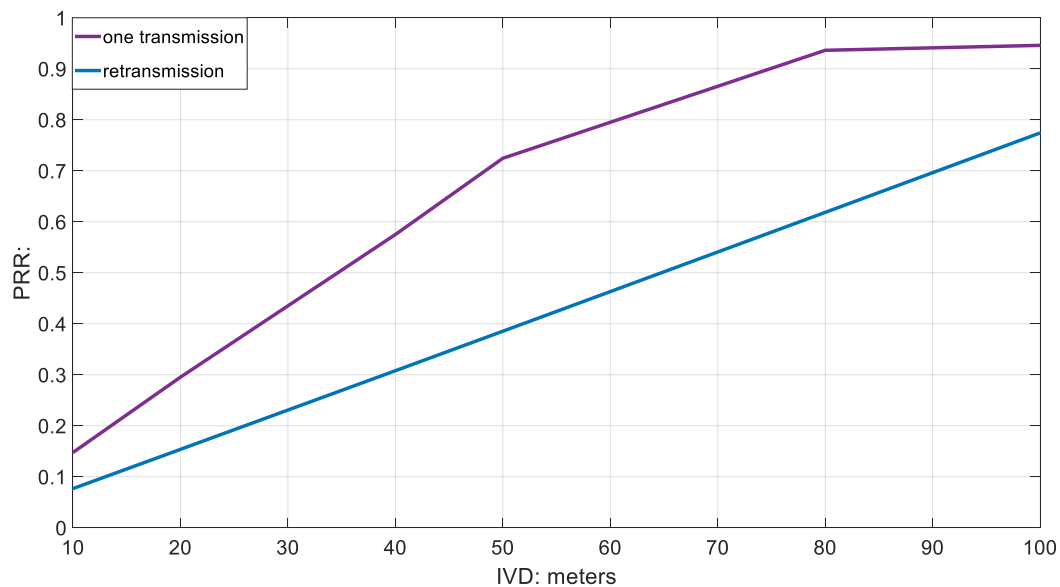| IVD/Velocity	#UEs on BS coverage	UE-supported	PRR_{max}	$PRR_{runtime}$	PRR
10	1039	80	0.0770	0.9970	0.0768
20	519	80	0.1541	0.9971	0.1537
40	259	80	0.3089	0.9966	0.3078
50	207	80	0.3865	0.9970	0.3853
80	129	80	0.6202	0.9971	0.6184
100	103	80	0.7767	0.9967	0.7740

Figure A-27: PRR Performance comparison for transmission and retransmission

In Figure A-27, the *PRR* comparison between transmission and retransmission for sidelink C-V2X communication has been plotted for a vehicle speed of 100 km/h.

As mentioned before, *PRR* is equal to the product of PRR_{max} and $PRR_{runtime}$. When retransmission is applied and the communication system is overloaded, then only 80 UEs are supported with retransmission. PRR_{max} values of the retransmission are smaller with retransmission compared to the values without retransmission. For example, when the 10-meter IVD is applied, PRR_{max} value is 7.7% with retransmission compared to 15.5% with one transmission. And the *PRR* value decreases from 14.8% without retransmitting data packets to 7.9% with retransmitting data packets.